Parametrized black hole quasinormal ringdown formalism for higher overtones

Shin'ichi Hirano,[1,2] Masashi Kimura,[3,2] Masahide Yamaguchi,[4,5] and Jiale Zhang[6,4]

[1]*Oyama National College of Technology, Oyama 323-0806, Japan*
[2]*Department of Physics, Rikkyo University, Toshima, Tokyo 171-8501, Japan*
[3]*Department of Information, Artificial Intelligence and Data Science, Daiichi Institute of Technology, Tokyo 110-0005, Japan*
[4]*Cosmology, Gravity, and Astroparticle Physics Group, Center for Theoretical Physics of the Universe, Institute for Basic Science (IBS), Daejeon, 34126, Korea*
[5]*Department of Physics, Tokyo Institute of Technology, Tokyo 152-8551, Japan*
[6]*Department of Physics, Graduate School of Humanities and Sciences, Ochanomizu University, Tokyo 112-8610, Japan*

(Received 25 April 2024; accepted 24 May 2024; published 9 July 2024)

We investigate the parametrized black hole quasinormal ringdown formalism, which is a robust framework used to analyze quasinormal modes in systems that closely resemble general relativity, paying particular attention to the higher overtones. We find that larger deviations from the general relativity case typically appear in the quasinormal frequencies for the higher overtones. This growing tendency for higher overtones can be understood using an analytical method, and its relations to previous works are briefly discussed. Our findings indicate that we can impose a strong constraint on gravity theories by considering the overtones of quasinormal modes.

DOI: 10.1103/PhysRevD.110.024015

I. INTRODUCTION

The direct detection of gravitational waves [1,2] has led to new perspectives in astrophysics, cosmology, and gravity. In the gravitational-wave signal of a binary black hole merger, the damped oscillation called the ringdown phase appears after the merger phase, signifying the process of stabilization of the final-state black hole. The spectrum of the ringdown phase is a superposition of damped sinusoids, or quasinormal modes (QNMs), that are uniquely determined by the remnant black hole's mass and spin in general relativity (GR). Through the examination of the ringdown gravitational-wave signal, one can estimate the mass and spin of the remnant black hole [3–5].

The QNMs in GR are labeled by three indices (ℓ, m, n), where $\ell \geq 2$, $-\ell \leq m \leq \ell$, and $n \geq 0$. Each set of the (ℓ, m) spheroidal-harmonic indices and the overtone n number corresponds to different modes. For each set of (ℓ, m), $n = 0$ modes denote the least-damped mode known as the fundamental mode, and there are an infinite number of overtones [6–8] with $n \geq 1$. The consistency with the ringdown phase with the $n = 0$ fundamental mode has been reported from real data [9–11]. In [12], it was suggested that overtones provide an excellent description of the waveform before the fundamental mode dominates and enable us to extend perturbation theory to times before the peak strain amplitude, yielding surprisingly good fits to numerical relativity simulations. This suggests the importance of including overtones in ringdown analysis, and many attempts have been made to fit numerical waveforms while acknowledging the existence of related and crucial arguments [13–40]. Numerous investigations in recent periods have been directed toward isolating QNMs from empirical measurements of gravitational waves [11,41–44]. Currently, the detection of overtones in real gravitational-wave data continues to be a subject of debate [13,14,45–51].

It is widely believed that inconsistencies of GR will eventually become evident in strong gravity regimes, such as near the curvature singularity, or large-scale descriptions [52,53]. This implies that the gravity theory should be modified from GR at some scale.[1] The test of gravity theories through ringdown phases can be carried out by comparing the spectra of the ringdown phase with the predictions made in GR or non-GR theories [53–57]. For this purpose, we utilize the methodology called the parametrized black hole quasinormal ringdown formalism (parametrized QNM formalism) [58], where quasinormal frequencies have minor deviations from the predictions of GR in configurations that are perturbatively close to GR. Note that while the form of this formalism assumes the

[1]Although one may assume that the Planck scale is the relevant scale, no one knows at what scale non-GR effects are important. Therefore, it is important to verify the theory of gravity from observations without being biased toward new scales.

Regge-Wheeler and Zerilli equations, which are master equations for the Schwarzschild case, as the lowest-order system, it can treat slowly rotating cases by considering the spin as a perturbative parameter [59].

In this paper, we study the parametrized black hole quasinormal ringdown formalism [58] for the higher overtones. To calculate the precise values of quasinormal frequencies, we adopt Nollert's method [60], which improves convergence over the larger imaginary parts while dealing with the computational difficulties with overtones. In contrast to the fundamental mode, we find a growing trend of the model-independent coefficients e_j in the parametrized QNM formalism [58] for higher overtones, which is consistent with the $n = 1, 2$ overtone cases [61]. Applying our results to typical modified gravity theories with higher-curvature correction terms, we confirm that the deviation of quasinormal frequencies from the predicted GR value is increased for higher overtones. We also briefly discuss the case of the algebraically special mode [62], i.e., $n = 8$ overtone with $\ell = 2$, and the relation with recent arguments related to the spectral instability of QNMs [63–67].

This paper is organized as follows. In Sec. II we review the framework of the parametrized QNM formalism along with the calculation methods we adopt. In Sec. III we show our numerical results for the calculation of the coefficients e_j in the parametrized QNM formalism for higher overtones. Our analysis reveals a notable trend: the parameter e_j increases with the overtone number n. This trend is evident in our numerical results and further supported by an analysis of the asymptotic behavior of the series e_j discussed in Sec. IV. In Sec. V we explore the implications of our results for some typical cases. In Appendix A recursion relations among the coefficients e_j are reviewed. In Appendix B we reveal a nontrivial relation including e_1. The discussion related to the algebraically special mode $\ell = 2$, $n = 8$ overtone is in Appendix C. The numerical results of the dimensionless Schwarzschild quasinormal frequencies and the coefficients e_j can be found in Appendices D and E.

II. PARAMETRIZED BLACK HOLE QUASINORMAL RINGDOWN FORMALISM AND CALCULATION METHOD

In this section, we briefly review the parametrized black hole quasinormal ringdown formalism (parametrized QNM formalism) from [58] and the calculation methods we adopt. We consider axial (odd-parity) gravitational perturbations whose master equation describes the small deviation from the Schwarzschild limit in the form

$$f\frac{d}{dr}\left(f\frac{d\Phi}{dr}\right)+(\omega^2-V)\Phi=0, \tag{1}$$

where $f = 1 - r_H/r$ and r_H denotes the location of the horizon. The effective potential V is given by

$$V = V_{\rm RW} + \delta V, \tag{2}$$

where $V_{\rm RW}$ is the Regge-Wheeler potential [68],

$$V_{\rm RW} = f\left(\frac{\ell(\ell+1)}{r^2}-\frac{3r_H}{r^3}\right), \tag{3}$$

with the notation ℓ used as an angular harmonic index to designate the tensorial spherical harmonics, and δV describes the small deviations from $V_{\rm RW}$ characterized by the small parameters α_j,

$$\delta V = \sum_{j=0}^{\infty}\delta V_j = \frac{f}{r_H^2}\sum_{j=0}^{\infty}\alpha_j\left(\frac{r_H}{r}\right)^j. \tag{4}$$

This parametrized potential includes many models [59,61,69–75], where different choices of the small parameters α_j correspond to the details of gravitational theories or physical setups (see also Sec. V for explicit examples).

The QNMs are the solutions of the master equation (1) that comply with the purely outgoing boundary condition at the spatial infinity ($r_* \to \infty$),[2]

$$\Phi \sim e^{i\omega r_*}, \tag{5}$$

and with the purely ingoing boundary condition at the horizon ($r_* \to -\infty$),

$$\Phi \sim e^{-i\omega r_*}, \tag{6}$$

where $r_* = r + r_H \ln(r - r_H)/r_H$. We note that these expressions incorporate the time dependency as $e^{-i\omega t}$. For the parametrized potentials (2)–(4), the corrections in the frequencies are linear in the corrections to the potentials. At the first order of small parameter $\mathcal{O}(\alpha_j)$, the quasinormal frequencies become [58]

$$\omega = \omega_{\rm Sch} + \sum_{j=0}^{\infty}\alpha_j e_j, \tag{7}$$

with

$$\omega_{\rm Sch} = \frac{2\Omega_{\rm Sch}}{r_H}, \tag{8}$$

where the coefficients e_j are constants, which are independent of α_j, and $\Omega_{\rm Sch}$ is the dimensionless Schwarzschild quasinormal frequency normalized by the mass, e.g., $\Omega_{\rm Sch} = 0.3736716844\cdots - i0.0889623157\cdots$ for $\ell = 2$, $n = 0$ (see Appendix D for other ℓ and n). To calculate the quasinormal frequencies in this paper, we employ Leaver's

[2]If the effective potential has a mass term with the mass squared μ^2, the boundary condition at $r_* \to \infty$ is changed into $\Phi \sim e^{i\sqrt{\omega^2-\mu^2}r_*}$. In that case, the ansatz of the wave function used in the series expansion (9) should also be modified.

method [76] as well as Nollert's improved method [60]. The wave function Φ in Eq. (1) can be expressed in series form as

$$\Phi = e^{i\omega r_*} f^{\rho} \sum_{k=0}^{\infty} a_k f^k, \tag{9}$$

where $\rho = -2ir_H\omega$ is the exponent satisfying the QNM boundary conditions at the horizon $r_* \to -\infty$ in the Frobenius method. The master equation can be reduced to recursion relations for the expansion coefficients a_k after performing some calculations. If a solution such that the summation in (9) at infinity is convergent, i.e., $\sum_{k=0}^{\infty} a_k$ is convergent, can be found, the QNM boundary condition at the spatial infinity $r_* \to \infty$ is simultaneously satisfied. Such frequencies that lead to convergent summation $\sum_{k=0}^{\infty} a_k$ are the quasinormal frequencies. We can find these frequencies using the so-called Leaver continuous fraction method with high accuracy, which is mathematically equivalent to solving the equation $a_K = 0$ for a large integer K. In fact, to obtain the quasinormal frequencies for higher overtones with high accuracy, we need Nollert's improved method, where we solve

$$\frac{a_K}{a_{K-1}} = \mathbf{c}_0 + \mathbf{c}_1 K^{-1/2} + \mathbf{c}_2 K^{-1} + \cdots \tag{10}$$

instead of $a_K = 0$. In Eq. (10), the coefficients $\mathbf{c}_i$ are determined from the asymptotic form of the recursion relation for a_k at large k with the convergence condition of the summation of a_k [60]. In Leaver's method we only impose that the summation of a_k is convergent, whereas in Nollert's method we also take into account the convergent rate of a_k. For this reason, solving Eq. (10) can give more accurate quasinormal frequencies than solving $a_K = 0$ for a fixed integer K. The technical details of Leaver's method and Nollert's method can be found in [77].

To determine the numerical value of e_j in Eq. (7), we use the perturbative calculation technique developed in [78], i.e., we solve Eq. (10) at the order $\mathcal{O}(\alpha_j)$ after substituting Eq. (7) into Eq. (10). The result is summarized in the next section.

III. RESULTS OF NUMERICAL CALCULATION FOR e_j

We calculated the precise numerical values of the coefficients of the parametrized QNM formalism e_j in Eq. (7) for higher overtones using Leaver's method [76] and Nollert's improved method [60]. The results of numerical calculations are detailed in Appendix E, with the case of $n = 8$ for $\ell = 2$ being a special scenario discussed in Appendix C. In Appendix D we also present the numerical values of quasinormal frequencies for Schwarzschild black holes. Our numerical data are available at the website [79].

We check the accuracy of our numerically calculated coefficients e_j by substituting them into Eq. (A1), the identical relations for e_j [80]. Defining the function of error estimation as

$$\Delta_{e_j} = \frac{|c_{j+1}e_{j+1} + c_{j+3}e_{j+3} + c_{j+4}e_{j+4} + c_{j+5}e_{j+5}|}{|c_{j+1}e_{j+1}| + |c_{j+3}e_{j+3}| + |c_{j+4}e_{j+4}| + |c_{j+5}e_{j+5}|}, \tag{11}$$

where c_{j+a} are given by Eqs. (A2)–(A5), we confirm that the margin of error Eq. (11) is at most $\mathcal{O}(10^{-21})$ for our numerical data of e_j.

Table I shows the typical values of e_j for the fundamental mode and overtones. While the absolute value of e_j for the

TABLE I. Typical numerical values of e_j. Cases for $\ell = 2$ and $n = 0$, 2, 10 are presented for various values of j.

$n = 0$	
j	$r_H e_j$
0	$0.24725 + 0.092643i$
1	$0.15985 + 0.018208i$
2	$0.096632 - 0.0024155i$
10	$0.0036853 + 0.0065244i$
15	$-0.00081238 + 0.0047307i$
20	$-0.0022183 + 0.0029672i$
25	$-0.0025952 + 0.0016658i$
50	$-0.0016013 - 0.00090149i$
75	$-0.00058591 - 0.0012547i$
100	$6.4338 \times 10^{-7} - 0.0011385i$
$n = 2$	
j	$r_H e_j$
0	$-0.006678 + 0.14146i$
1	$0.11931 + 0.075616i$
2	$0.11467 + 0.00074885i$
10	$0.048075 + 0.052281i$
15	$0.029569 + 0.081252i$
20	$0.0057647 + 0.10267i$
25	$-0.021305 + 0.11745i$
50	$-0.16315 + 0.11792i$
75	$-0.27727 + 0.045252i$
100	$-0.35334 - 0.061499i$
$n = 10$	
j	$r_H e_j$
0	$-0.028643 + 0.010611i$
1	$-0.044125 + 0.046418i$
2	$-0.075205 + 0.046894i$
10	$-11.971 + 1.9125i$
15	$-82.298 + 9.0573i$
20	$-390.83 + 28.087i$
25	$-1459.5 + 57.673i$
50	$-1.5199 \times 10^5 - 12603i$
75	$-3.1869 \times 10^6 - 5.4383 \times 10^5 i$
100	$-3.0889 \times 10^7 - 7.4294 \times 10^6 i$

fundamental mode ($n = 0$) decays as j increases, it grows for overtones as j increases in the large-j regime. This suggests that higher-overtone modes are much more sensitive to modifications in the effective potential, which is consistent with [61]. The growing trend of the coefficients e_j for large j in overtones can be understood from the asymptotic analysis, as discussed in the next section.

IV. ASYMPTOTIC BEHAVIOR OF e_j FOR LARGE j

In this section, we discuss the asymptotic behavior of the coefficients e_j for large j. As discussed in Appendix A, the coefficients e_j satisfy the recursion relations in Eq. (A1). By defining the ratio of e_j and e_{j-1} as $b_j := e_j/e_{j-1}$, Eq. (A1) has an approximate solution for large j in the Taylor series as

$$b_j = \frac{e_j}{e_{j-1}} = 1 + \sum_{i=1}^{\infty} \frac{C_i}{j^i}, \tag{12}$$

where C_i are constants that capture the behavior of the series. The explicit forms of C_i with lower indices i are[3]

$$C_1 = i(i + 2r_H\omega_{\rm Sch}), \tag{13}$$

$$C_2 = -C_1^2 - 2(-3 + \ell + \ell^2), \tag{14}$$

$$C_3 = 2C_1^3 - 6(-3 + \ell + \ell^2) + \frac{2(-3 + \ell + \ell^2)^2}{C_1} + C_1(-1 + 2\ell(1 + \ell)), \tag{15}$$

$$C_4 = C_1^3 - 5C_1^4 - 38(-3 + \ell + \ell^2) + \frac{18(-3 + \ell + \ell^2)^2}{C_1} - 2C_1^2(-5 + 3\ell + 3\ell^2) + C_1(-1 + 6\ell + 6\ell^2),$$

$$\begin{aligned} C_5 = {} & \frac{1}{(-1 + C_1)C_1^2}\big(-21C_1^7 + 14C_1^8 - 2(-3 + \ell + \ell^2)^4 - 14C_1^5(-5 + 3\ell + 3\ell^2) \\ & + 4C_1^6(-8 + 5\ell + 5\ell^2) - 2C_1(-3 + \ell + \ell^2)^2(55 + 6\ell + 6\ell^2) \\ & - 2C_1^3(-284 + 103\ell + 106\ell^2 + 6\ell^3 + 3\ell^4) + C_1^4(-23 + 30\ell + 36\ell^2 + 12\ell^3 + 6\ell^4) \\ & - 2C_1^2(-252 + 309\ell + 228\ell^2 - 160\ell^3 - 75\ell^4 + 6\ell^5 + 2\ell^6)\big), \end{aligned} \tag{16}$$

$$\begin{aligned} C_6 = {} & -\frac{1}{(-1 + C_1)C_1^2}\big(-79C_1^8 + 42C_1^9 + 32(-3 + \ell + \ell^2)^4 + 35C_1^7(-3 + 2\ell + 2\ell^2) \\ & - 4C_1^6(-77 + 41\ell + 41\ell^2) + 2C_1(-3 + \ell + \ell^2)^2(277 + 96\ell + 96\ell^2) \\ & + C_1^5(-173 + 64\ell + 96\ell^2 + 64\ell^3 + 32\ell^4) - 2C_1^4(10 - 22\ell + 17\ell^2 + 78\ell^3 + 39\ell^4) \\ & + C_1^3(-2643 + 960\ell + 1010\ell^2 + 100\ell^3 + 50\ell^4) \\ & + 2C_1^2(-1878 + 2423\ell + 1728\ell^2 - 1358\ell^3 - 599\ell^4 + 96\ell^5 + 32\ell^6)\big), \end{aligned} \tag{17}$$

[3]Since Eq. (A1) represents a five-term recursion relation, the general solution is described by a superposition of four fundamental solutions. The fundamental solution, which becomes the leading term in the general solution for large j, satisfies the ansatz (12) with Eq. (13). We note that the contribution of the other three solutions is subdominant in the large-j regime compared to the solution (12) with Eq. (13).

$$
\begin{aligned}
C_7 = \frac{1}{(-2+C_1)(-1+C_1)C_1^3}\big(&-572C_1^{11}+132C_1^{12}+4(-3+\ell+\ell^2)^6\\
&+8C_1(-3+\ell+\ell^2)^4(76+5\ell+5\ell^2)+4C_1^{10}(74+63\ell+63\ell^2)-4C_1^9(-493+295\ell+295\ell^2)\\
&+2C_1^8(-1752+778\ell+853\ell^2+150\ell^3+75\ell^4)-2C_1^7(-695-200\ell+162\ell^2+724\ell^3+362\ell^4)\\
&+4C_1^2(-3+\ell+\ell^2)^2(487+1491\ell+1414\ell^2-151\ell^3-68\ell^4+9\ell^5+3\ell^6)\\
&+C_1^6(967-2346\ell-1034\ell^2+2644\ell^3+1372\ell^4+60\ell^5+20\ell^6)\\
&-C_1^5(-10725+2772\ell+4016\ell^2+2540\ell^3+1400\ell^4+156\ell^5+52\ell^6)\\
&-2C_1^4(-1416+12583\ell+7095\ell^2-10678\ell^3-4594\ell^4+894\ell^5+298\ell^6)\\
&+2C_1^3(-34911+32394\ell+27233\ell^2-11040\ell^3-7271\ell^4-1978\ell^5-454\ell^6+176\ell^7+44\ell^8)\big).
\end{aligned}
\tag{18}
$$

Equation (12) can be solved with respect to e_j as

$$
e_j \simeq C e^{A_1 \ln j - 1 + P(j)},
\tag{19}
$$

where C is a constant and the function $P(j)$ is given by

$$
P(j) = 1 + \sum_{i=1}^{\infty} \frac{A_{i+1}}{j^i},
\tag{20}
$$

wherein the coefficients A_i can be defined through their correlations with C_i:

$$
A_1 = C_1,
\tag{21}
$$

$$
A_2 = \frac{1}{2}(C_1 + C_1^2 - 2C_2),
\tag{22}
$$

$$
A_3 = -\frac{1}{12}(1+C_1)(C_1+2C_1^2-6C_2) - \frac{C_3}{2},
\tag{23}
$$

$$
A_4 = \frac{1}{12}\big(2C_1^3 + C_1^4 + C_1^2(1-4C_2) + 2(-1+C_2)C_2 + 6C_3 + C_1(-6C_2+4C_3) - 4C_4\big),
\tag{24}
$$

$$
\begin{aligned}
A_5 = \frac{1}{120}\big(&-15C_1^4 - 6C_1^5 + 10C_1^3(-1+3C_2) + 30C_1^2(2C_2 - C_3)\\
&+ C_1(1 - 30(-1+C_2)C_2 - 60C_3 + 30C_4) - 30(C_2^2 + C_3 - C_2C_3 - 2C_4 + C_5)\big),
\end{aligned}
\tag{25}
$$

$$
\begin{aligned}
A_6 = \frac{1}{60}\big(&6C_1^5 + 2C_1^6 + C_1^4(5-12C_2) + 6C_1^3(-5C_2+2C_3) + C_1^2\big(-1+2C_2(-10+9C_2)+30C_3-12C_4\big)\\
&+ 2C_1(3C_2(5C_2-4C_3)+10C_3-15C_4+6C_5)\\
&+ 2(C_2 + 5C_2^2 - 2C_2^3 - 15C_2C_3 + 3C_3^2 - 10C_4 + 6C_2C_4 + 15C_5 - 6C_6)\big),
\end{aligned}
\tag{26}
$$

$$
\begin{aligned}
A_7 = \frac{1}{252}\big(&-21C_1^6 - 6C_1^7 + 21C_1^5(-1+2C_2) + 42C_1^4(3C_2 - C_3)\\
&+ 7C_1^3\big(1 + 3(5-4C_2)C_2 - 18C_3 + 6C_4\big) - 21C_1^2\big(9C_2^2 + 5C_3 - 6C_2C_3 - 6C_4 + 2C_5\big)\\
&+ C_1\big(-1 + 21\big(-5C_2^2 + 2C_2^3 - 2C_3^2 + C_2(-1+12C_3-4C_4)\big) + 105C_4 - 126C_5 + 42C_6\big)\\
&+ 21\big(2C_2^3 + C_3 - 2C_2^2C_3 - 3C_3^2 + 2C_3C_4 - 5C_5 + C_2(5C_3 - 6C_4 + 2C_5) + 6C_6 - 2C_7\big)\big).
\end{aligned}
\tag{27}
$$

Hence, the leading term of e_j becomes[4]

$$e_j \simeq e_j^{\text{Leading}} = Ce^{A_1 \ln j} = Cj^{-1-2r_H\omega_I} e^{2ir_H\omega_R \ln j}, \quad (28)$$

where $\omega_{\text{Sch}} = \omega_R + i\omega_I$. This coincides with the asymptotic form of e_j estimated in [58]. This demonstrates that the factor $j^{-1-2r_H\omega_I}$ determines the convergence or divergence of $|e_j|$ for large j. In the top three columns of Table II, we display the values of $j^{-1-2r_H\omega_I}$ for $\ell = 2, 3, 4$ across various overtone numbers n. For the fundamental mode, $|e_j|$ shows a decreasing trend at $j \to \infty$; yet, it shows divergence for overtones. This indicates that the correction to the QNM frequency $\alpha_j e_j$, as outlined in Eq. (7), contributes significantly to overtones at large j.

Let us consider the physical implications of our results. For large j, δV_j in Eq. (4) has a peak near the horizon

$$r_* = -r_H \ln(j/e), \quad (29)$$

since δV_j for large j near the peak can be written in the form

$$\delta V_j = f\frac{\alpha_j}{r_H^2}\left(\frac{r_H}{r}\right)^j \simeq \frac{1}{er_H^2}\frac{\alpha_j}{j} e^{-(r_*+r_H\ln(j/e))^2/(2r_H^2)}, \quad (30)$$

as demonstrated in [58]. This indicates that the large-j limit corresponds to modifications to the effective potential in the near-horizon regime. On the other hand, we confirm the increasing trend of e_j for overtones as j increases, in contrast to the fundamental mode where e_j decays as j increases.[5] Thus, we conclude that near-horizon modifications of the effective potential strongly influence the overtones of QNMs, but not the fundamental mode. This is consistent with results in [67] which stated that the first few overtones are capable of probing the geometry close to the event horizon. Also, our result provides a partial answer to the recently confirmed findings that the overtone spectra are relatively more unstable against perturbations in the effective potential compared to the fundamental mode [63–66].

For the large-ℓ case, it is known that the first-order WKB formula from [81],

$$\omega_{\text{Sch}} \simeq \omega_{\text{WKB}} = \frac{2}{3\sqrt{3}r_H}\left(\ell + \frac{1}{2} - i\left(n + \frac{1}{2}\right)\right) + \mathcal{O}(1/\ell), \quad (31)$$

TABLE II. Values of $j^{-1-2r_H\omega_I}$ for $\ell = 2, 3, 4$ and the WKB formula across various overtone numbers n. The WKB formula in Eq. (31) corresponds to the approximation for large ℓ.

$\ell = 2$	
n	$j^{-1-2r_H\omega_I}$
0	$j^{-0.64415074}$
1	$j^{0.095659501}$
2	$j^{0.91310793}$
3	$j^{1.8205928}$
4	$j^{2.7873796}$
5	$j^{3.7824322}$
6	$j^{4.7916425}$
7	$j^{5.8153647}$
$\ell = 3$	
n	$j^{-1-2r_H\omega_I}$
0	$j^{-0.62918781}$
1	$j^{0.12519245}$
2	$j^{0.91637100}$
3	$j^{1.7613484}$
4	$j^{2.6625976}$
5	$j^{3.6086054}$
6	$j^{4.5836490}$
7	$j^{5.5753781}$
$\ell = 4$	
n	$j^{-1-2r_H\omega_I}$
0	$j^{-0.62334416}$
1	$j^{0.13733740}$
2	$j^{0.91963270}$
3	$j^{1.7356973}$
4	$j^{2.5929559}$
5	$j^{3.4919070}$
6	$j^{4.4267451}$
7	$j^{5.3886827}$
WKB (large ℓ)	
n	$j^{-1-2r_H\omega_I}$
0	$j^{-0.61509982}$
1	$j^{0.15470054}$
2	$j^{0.92450090}$
3	$j^{1.6943013}$
4	$j^{2.4641016}$
5	$j^{3.2339020}$
6	$j^{4.0037023}$
7	$j^{4.7735027}$

[4]Equation (28) is valid for any value of the overtone number n and the angular harmonic index ℓ as long as j is sufficiently large.

[5]If we define $\tilde{\alpha}_j := \alpha_j/j$ and $\tilde{e}_j := je_j$ for $j \geq 1$, the amplitude of δV_j in Eq. (30) is proportional to $\tilde{\alpha}_j$, and the modification to the quasinormal frequency in Eq. (7) becomes $\sum_j \alpha_j e_j = \sum_j \tilde{\alpha}_j \tilde{e}_j$. From Eq. (28), $\tilde{e}_j$ for large j behaves as $\tilde{e}_j \simeq Cj^{-2r_H\omega_I} e^{2ir_H\omega_R \ln j}$. While the factor $j^{-2r_H\omega_I}$ grows as j increases for both the fundamental mode and overtones, the factor for the fundamental mode is still relatively smaller than that for the overtones.

provides a good approximation of the quasinormal frequency for the Schwarzschild black hole. In the bottom column of Table II we also show the value of $j^{-1-2r_H\omega_I}$ for the WKB formula using Eq. (31). We observe that the trend is consistent with the cases involving lower ℓ values.

To extend the validity of the approximate solution (19) with Eq. (20) for large j to lower values of j, we apply the Padé approximants to the function $P(j)$ up to j^{-6} order, which can be written as follows:

$$P^{[3/3]} = \frac{\tilde{A}_0 + \tilde{A}_1/j + \tilde{A}_2/j^2 + \tilde{A}_3/j^3}{1 + \tilde{B}_1/j + \tilde{B}_2/j^2 + \tilde{B}_3/j^3}, \tag{32}$$

where the coefficients $\tilde{A}_i, \tilde{B}_i$ are selected so that the Taylor series of Eq. (32) matches that of $P(j)$ in Eq. (20) up to j^{-6}. Replacing $P(j)$ in Eq. (19) with $P^{[3/3]}$, we obtain the approximate expression

$$e_j^{\text{Padé}} = Ce^{A_1 \ln j - 1 + P^{[3/3]}}. \tag{33}$$

Table III shows values of e_j/e_{j-1} for our numerical results, e_j^{Leading} in Eq. (28), and $e_j^{\text{Padé}}$ in Eq. (33), in the cases $\ell = 2$, $n = 2$, 10.

Both the approximate expressions derived from the leading behavior and the Padé approximants are consistent with the numerical results for large values of j. However, only the Padé approximants exhibit a high level of agreement with the numerical results even for small values of j. We confirm that the same tendency can be observed across various values of the angular harmonic index ℓ and overtone numbers n.

In the above discussion, we showed that $|e_j|$ with high j increases for higher overtones. This raises the question of whether the quasinormal frequencies are still described by small corrections to the GR case. Therefore, we comment on the validity of the parametrized QNM formalism in Eq. (7). For the parametrized potential in Eq. (4), the quasinormal frequency ω is described by the function of the parameters α_j. Assuming that the quasinormal frequency ω can be expanded in a Taylor series of α_j, we obtain Eq. (7) by taking up to the first order. The first-order approximation (7) is a good approximation if

$$|\omega_{\text{Sch}}| \gg \sum_{j=0}^{\infty} |\alpha_j e_j| \tag{34}$$

is satisfied. Thus, as far as we consider sufficiently small parameters α_j, the expansion in Eq. (7) is still a good approximation even if $|e_j|$ takes very large values.

On the other hand, if we consider fixed values of the parameters α_j, even though the expansion in Eq. (7) is valid for lower overtones, we should not expect it to be a good approximation for higher overtones. The threshold of the validity of the expansion in Eq. (7) can be estimated by finding overtone number n, which gives

$$|\omega_{\text{Sch}}| \sim \sum_{j=0}^{\infty} |\alpha_j e_j|. \tag{35}$$

In the next section, we discuss the threshold for some examples.

TABLE III. Values of e_j/e_{j-1} for $\ell = 2$ with different overtone numbers n.

$n = 2$			
j	Numerics	Leading	Padé
3	$0.6820 - 0.1190i$	$1.279 + 0.679i$	$0.2616 + 0.4728i$
4	$0.7421 + 0.1408i$	$1.2232 + 0.4415i$	$0.7046 + 0.2915i$
5	$0.9493 + 0.2468i$	$1.1820 + 0.3255i$	$0.8791 + 0.2180i$
6	$1.0484 + 0.1552i$	$1.1528 + 0.2572i$	$0.9586 + 0.1835i$
7	$1.0341 + 0.1073i$	$1.1314 + 0.2125i$	$1.0012 + 0.1603i$
8	$1.0221 + 0.1034i$	$1.1151 + 0.1809i$	$1.0253 + 0.1392i$
9	$1.0244 + 0.1050i$	$1.1024 + 0.1574i$	$1.0368 + 0.1200i$
10	$1.0309 + 0.1016i$	$1.0921 + 0.1393i$	$1.0404 + 0.1049i$
11	$1.0355 + 0.0948i$	$1.0838 + 0.1249i$	$1.0405 + 0.0941i$
12	$1.0375 + 0.0875i$	$1.0768 + 0.1132i$	$1.0396 + 0.0862i$
13	$1.0377 + 0.0810i$	$1.0708 + 0.1035i$	$1.0385 + 0.0800i$
14	$1.0372 + 0.0756i$	$1.0658 + 0.0954i$	$1.0374 + 0.0750i$
15	$1.0363 + 0.0710i$	$1.0614 + 0.0884i$	$1.0364 + 0.0706i$
16	$1.0354 + 0.0670i$	$1.0575 + 0.0824i$	$1.0354 + 0.0668i$
17	$1.0344 + 0.0635i$	$1.0541 + 0.0771i$	$1.0344 + 0.0634i$
18	$1.0335 + 0.0603i$	$1.0511 + 0.0725i$	$1.0335 + 0.0603i$
19	$1.0325 + 0.0575i$	$1.0484 + 0.0684i$	$1.0325 + 0.0574i$
20	$1.0316 + 0.0549i$	$1.0460 + 0.0647i$	$1.0316 + 0.0549i$
$n = 10$			
j	Numerics	Leading	Padé
3	$2.431 + 0.955i$	$42.10 + 5.25i$	$4.048 + 0.268i$
4	$2.251 - 0.103i$	$14.23 + 1.26i$	$2.570 + 0.096i$
5	$1.807 - 0.020i$	$7.848 + 0.537i$	$2.111 + 0.053i$
6	$1.772 + 0.107i$	$5.385 + 0.301i$	$1.895 + 0.035i$
7	$1.781 + 0.040i$	$4.153 + 0.196i$	$1.768 + 0.027i$
8	$1.674 - 0.024i$	$3.433 + 0.140i$	$1.683 + 0.022i$
9	$1.578 - 0.006i$	$2.968 + 0.107i$	$1.619 + 0.019i$
10	$1.539 + 0.026i$	$2.647 + 0.085i$	$1.570 + 0.017i$
11	$1.525 + 0.029i$	$2.412 + 0.070i$	$1.530 + 0.015i$
12	$1.501 + 0.016i$	$2.234 + 0.060i$	$1.496 + 0.014i$
13	$1.467 + 0.008i$	$2.095 + 0.051i$	$1.466 + 0.013i$
14	$1.437 + 0.008i$	$1.983 + 0.045i$	$1.441 + 0.012i$
15	$1.415 + 0.011i$	$1.892 + 0.040i$	$1.418 + 0.012i$
16	$1.3964 + 0.0119i$	$1.815 + 0.036i$	$1.3984 + 0.0110i$
17	$1.3797 + 0.0112i$	$1.751 + 0.033i$	$1.3803 + 0.0105i$
18	$1.3638 + 0.0101i$	$1.696 + 0.030i$	$1.3640 + 0.0101i$
19	$1.3488 + 0.0095i$	$1.648 + 0.027i$	$1.3491 + 0.0097i$
20	$1.3351 + 0.0091i$	$1.606 + 0.025i$	$1.3354 + 0.0093i$

V. APPLICATIONS

In this section, we apply our formalism to typical gravity theories with higher-curvature correction terms and consider the slowly rotating Kerr black hole cases.

A. Effective field theory extension of GR

The analysis of black hole models developed within the framework of effective field theory (EFT), as discussed in the studies [71,82–91]. References [82] and [83] are representative examples in this context to investigate our formalism, where the model differs from GR through three coupling constants that determine the extent of modifications at high curvature levels. For simplicity, our discussion will be limited to a single coupling constant, represented as $\tilde{\Lambda}$ (equivalently referred to as ϵ_2 in [83], whose notation we adopt). Within this framework, nonspinning black holes are described by the Schwarzschild metric, and their axial gravitational perturbations yield a modified master equation,

$$f\frac{d}{dr}\left(f\frac{d\Phi}{dr}\right)+[\omega^2-(V_{\rm RW}+\delta V)]\Phi=0, \quad (36)$$

where $f=1-r_H/r$ and $V_{\rm RW}$ is given by Eq. (3), while the extra term in the effective potential reads

$$\delta V=f\frac{18(\ell+2)(\ell+1)\ell(\ell-1)r_H^8}{r^{10}}\epsilon_2. \quad (37)$$

The only coefficient of the expansion (4) in Sec. II is then

$$\alpha_{10}=18(\ell+2)(\ell+1)\ell(\ell-1)\epsilon_2. \quad (38)$$

Thus, the quasinormal frequencies are expressed as

$$\begin{aligned}\omega&=\omega_{\rm Sch}+\alpha_{10}e_{10}\\&=\frac{\Omega_{\rm Sch}}{M}+18(\ell+2)(\ell+1)\ell(\ell-1)\epsilon_2 e_{10},\end{aligned} \quad (39)$$

where we used that $\omega_{\rm Sch}$ is given by Eq. (8) and $r_H=2M$. Table IV shows the quasinormal frequencies for EFT with $\ell=2$, 3. A significant deviation from the predictions of GR in both the real and imaginary parts can be observed in higher overtones. We report that the same trend is confirmed for $\ell=4$, 5, 6 cases.

We note that $\epsilon_2\lesssim\mathcal{O}(1)$ in the observational constraints [87,92] and theoretical arguments [91,93–96]. For the validity of the expansion in Eq. (7), Eq. (34) should be satisfied. For example, if we set $\epsilon_2=10^{-5}$, Eq. (35) holds for $n=7$ and $\ell=2$ in Table IV. This implies that the expansion in Eq. (7) is a good approximation for $n\leq 7$ and $\ell=2$ if $\epsilon_2\ll 10^{-5}$.

TABLE IV. Quasinormal frequencies in EFT (with ϵ_2 dependency).

$\ell=2$	
n	$2M\omega$
0	$0.74734-0.17792i+(1.5921+2.8186i)\epsilon_2$
1	$0.69342-0.54783i+(6.2213+10.0684i)\epsilon_2$
2	$0.60211-0.95655i+(20.768+22.585i)\epsilon_2$
3	$0.50301-1.4103i+(58.262+45.413i)\epsilon_2$
4	$0.41503-1.8937i+(147.49+87.27i)\epsilon_2$
5	$0.33860-2.3912i+(356.32+168.61i)\epsilon_2$
6	$0.26650-2.8958i+(877.52+355.27i)\epsilon_2$
7	$0.18564-3.4077i+(2541.0+1005.3i)\epsilon_2$
8	$-4i+(1.6745\times10^5 i)\epsilon_2$
9	$0.12653-4.6053i-(6593.9-1682.1i)\epsilon_2$
10	$0.15311-5.1217i-(5171.6-826.2i)\epsilon_2$

$\ell=3$	
n	$2M\omega$
0	$1.19889-0.18541i+(5.0706+5.6488i)\epsilon_2$
1	$1.16529-0.56260i+(10.336+18.267i)\epsilon_2$
2	$1.1034-0.9582i+(23.240+34.872i)\epsilon_2$
3	$1.0239-1.3807i+(48.491+58.146i)\epsilon_2$
4	$0.9403-1.8313i+(93.205+90.609i)\epsilon_2$
5	$0.8628-2.3043i+(167.27+134.50i)\epsilon_2$
6	$0.7953-2.7918i+(283.77+191.88i)\epsilon_2$
7	$0.7380-3.2877i+(459.23+264.76i)\epsilon_2$
8	$0.6892-3.7881i+(714.04+355.10i)\epsilon_2$
9	$0.6474-4.2908i+(1073.01+464.75i)\epsilon_2$
10	$0.6109-4.7947i+(1566.0+595.5i)\epsilon_2$

B. Scalar Gauss-Bonnet gravity

In this subsection, we discuss the case of scalar Gauss-Bonnet (sGB) gravity [97–104]. sGB gravity is a typical model of modified gravity with a single scalar field, and it is also recognized as a low-energy effective theory that emerges from string theory [100–103]. Adopting the notation from [105], the Lagrangian for shift-symmetric sGB gravity is given by

$$\mathcal{L}=\frac{M_{\rm Pl}^2}{2}R-\frac{1}{2}(\partial\phi)^2+\frac{b_1}{\Lambda}\phi\left(R^2-4R_{\mu\nu}R^{\mu\nu}+R_{\mu\nu\rho\sigma}R^{\mu\nu\rho\sigma}\right), \quad (40)$$

where $M_{\rm Pl}$ is the Planck mass, Λ is the cutoff scale, and b_1 is the coupling constant. In the case of weak coupling, the sGB term is treated as a correction, so we can obtain the contribution of the sGB term to the GR values perturbatively.

Let us consider static spherically symmetric black hole solutions. The sGB term allows the scalar field to acquire a background value [106]. Consequently, the metric changes from the Schwarzschild one. For example, the horizon scale r_H departs from the Schwarzschild radius,

$$r_H = 2M\left(1 - \epsilon^2 b_1^2 \frac{98}{5}\right), \tag{41}$$

where M is the Arnowitt-Deser-Misner mass and $\epsilon = 1/(4\Lambda M_{\rm Pl} M^2)$ is a small parameter. The master equation governing the axial gravitational perturbations around the static spherically symmetric solutions is modified by the sGB correction [105], which can be expressed as

$$f\frac{d}{dr}\left(f\frac{d\Phi}{dr}\right) + [\tilde{\omega}^2 - (V_{\rm RW} + \delta V)]\Phi = 0, \tag{42}$$

where $f = 1 - r_H/r$ and

$$\tilde{\omega}^2 = \left(1 + \frac{4b_1^2\epsilon^2}{15}\right)\omega^2, \tag{43}$$

$$\begin{aligned}\delta V = f\Bigg[&\frac{4b_1^2\epsilon^2\omega^2}{15r^5}\left(r^5 - 146r^4 r_H - 263r^3 r_H^2 - 120r^2 r_H^3 + 98r r_H^4 + 340 r_H^5\right)\\ &+ \frac{b_1^2\epsilon^2}{15r^9} r_H\{294(-4 + \ell + \ell^2)r^6 + 87(-9 + 2\ell + 2\ell^2)r^5 r_H\\ &- 6(-1825 + 221\ell + 221\ell^2)r^4 r_H^2 - (647 + 646\ell + 646\ell^2)r^3 r_H^3\\ &- 676(-6 + \ell + \ell^2)r^2 r_H^4 + 10(-6601 + 218\ell + 218\ell^2) r r_H^5 + 56400 r_H^6\}\Bigg].\end{aligned} \tag{44}$$

The expansion coefficients in Eq. (4) can be obtained by reading off from the potential term (44) up to order ϵ^2:

$$\alpha_0 = \frac{4}{15} b_1^2\epsilon^2 r_H^2\omega^2, \tag{45}$$

$$\alpha_1 = -\frac{584}{15} b_1^2\epsilon^2 r_H^2\omega^2, \tag{46}$$

$$\alpha_2 = -\frac{1052}{15} b_1^2\epsilon^2 r_H^2\omega^2, \tag{47}$$

$$\alpha_3 = \frac{2}{5} b_1^2\epsilon^2\left(-196 + 49\ell + 49\ell^2 - 80 r_H^2\omega^2\right), \tag{48}$$

$$\alpha_4 = \frac{1}{15} b_1^2\epsilon^2\left(-783 + 174\ell + 174\ell^2 + 392 r_H^2\omega^2\right), \tag{49}$$

$$\alpha_5 = \frac{2}{15} b_1^2\epsilon^2\left(5475 - 663\ell - 663\ell^2 + 680 r_H^2\omega^2\right), \tag{50}$$

$$\alpha_6 = -\frac{1}{15} b_1^2\epsilon^2(647 + 646\ell + 646\ell^2), \tag{51}$$

$$\alpha_7 = -\frac{676}{15} b_1^2\epsilon^2(-6 + \ell + \ell^2), \tag{52}$$

$$\alpha_8 = \frac{2}{3} b_1^2\epsilon^2(-6601 + 218\ell + 218\ell^2), \tag{53}$$

$$\alpha_9 = 3760 b_1^2\epsilon^2. \tag{54}$$

The parametrized QNM formalism is applied to the renormalized $\tilde{\omega}$ in Eq. (43). The quasinormal frequencies are given by

$$\begin{aligned}\omega &= \left(1 - \frac{2b_1^2}{15}\epsilon^2\right)\omega_{\rm Sch} + \sum_{j=0}^{9}\alpha_j e_j + \mathcal{O}(\epsilon^4)\\ &= \frac{\Omega_{\rm Sch}}{M} + \frac{b_1^2\epsilon^2}{15M}\left[292\Omega_{\rm Sch} + 16M\Omega_{\rm Sch}^2(e_0 - 146e_1 - 263e_2 - 120e_3 + 98e_4 + 340e_5)\right.\\ &\quad + M(-783e_4 + 10950e_5 - 647e_6 + 4056e_7 - 66010e_8 + 56400e_9 + 294e_3(\ell^2 + \ell - 4)\\ &\quad \left. + 2\ell(\ell + 1)(87e_4 - 663e_5 - 323e_6 - 338e_7 + 1090e_8))\right] + \mathcal{O}(\epsilon^4).\end{aligned} \tag{55}$$

TABLE V. Quasinormal frequencies in sGB gravity for various ℓ values.

$\ell = 2$	
n	$2M\omega$
0	$0.74734 - 0.17792i + (14.548 - 3.464i)b_1^2\epsilon^2$
1	$0.69342 - 0.54783i + (13.499 - 10.664i)b_1^2\epsilon^2$
2	$0.60211 - 0.95655i + (11.721 - 18.621i)b_1^2\epsilon^2$
3	$0.5030 - 1.4103i + (9.792 - 27.454i)b_1^2\epsilon^2$
4	$0.4150 - 1.8937i + (8.079 - 36.864i)b_1^2\epsilon^2$
5	$0.3386 - 2.3912i + (6.591 - 46.549i)b_1^2\epsilon^2$
6	$0.2665 - 2.8958i + (5.188 - 56.372i)b_1^2\epsilon^2$
7	$0.1856 - 3.4077i + (3.614 - 66.336i)b_1^2\epsilon^2$
8	$-4i - (77.867i)b_1^2\epsilon^2$
9	$0.1265 - 4.6053i + (2.463 - 89.650i)b_1^2\epsilon^2$
10	$0.1531 - 5.1217i + (2.980 - 99.702i)b_1^2\epsilon^2$
$\ell = 3$	
n	$2M\omega$
0	$1.19889 - 0.18541i + (23.338 - 3.609i)b_1^2\epsilon^2$
1	$1.16529 - 0.56260i + (22.684 - 10.952i)b_1^2\epsilon^2$
2	$1.1034 - 0.9582i + (21.479 - 18.653i)b_1^2\epsilon^2$
3	$1.0239 - 1.3807i + (19.932 - 26.877i)b_1^2\epsilon^2$
4	$0.9403 - 1.8313i + (18.305 - 35.649i)b_1^2\epsilon^2$
5	$0.8628 - 2.3043i + (16.795 - 44.857i)b_1^2\epsilon^2$
6	$0.7953 - 2.7918i + (15.482 - 54.348i)b_1^2\epsilon^2$
7	$0.7380 - 3.2877i + (14.366 - 64.000i)b_1^2\epsilon^2$
8	$0.6892 - 3.7881i + (13.417 - 73.741i)b_1^2\epsilon^2$
9	$0.6474 - 4.2908i + (12.602 - 83.528i)b_1^2\epsilon^2$
10	$0.6109 - 4.7947i + (11.893 - 93.337i)b_1^2\epsilon^2$

The resultant quasinormal frequencies for $\ell = 2$ and $\ell = 3$ are listed in Table V. The imaginary part of the quasinormal frequencies in sGB gravity has a growing trend as the overtone number becomes higher.

The observational constraints [87,92] and theoretical arguments [91,93–96] imply $b_1^2\epsilon^2 \lesssim \mathcal{O}(1)$. For the expansion in Eq. (7) to be valid, Eq. (34) should be satisfied. For example, considering $b_1^2\epsilon^2 = 10^{-2}$, Eq. (35) holds for $n = 10$ and $\ell = 2$ in Table V. Therefore, if $b_1^2\epsilon^2 \ll 10^{-2}$, the expansion in Eq. (7) is a good approximation for $n \leq 10$ and $\ell = 2$.

C. Slowly rotating Kerr black holes

In this subsection, we present a comparison between numerical results [107,108] and the first-order semianalytic expression of QNMs for slowly rotating Kerr black holes, as we briefly demonstrate how the parametrized QNM formalism can be used to derive the semianalytic QNM frequency of the Kerr black hole.

The Chandrasekhar-Detweiler equation [109,110], derived from the Teukolsky equation [7] through variable transformations, reduces to the Regge-Wheeler equation in the Schwarzschild limit. As detailed in [59], for slowly rotating cases, the Chandrasekhar-Detweiler equation can be rewritten in a form such that the parametrized QNM formalism is applicable,

$$f\frac{d}{dr}\left(f\frac{d}{dr}\right)\Phi + \left(\left(\omega - \frac{m}{r_H}\sqrt{\frac{r_-}{r_H}}\right)^2 - (V_{\rm RW} + \delta V)\right)\Phi = 0, \tag{56}$$

where $f = 1 - r_H/r$, $r_H = M + \sqrt{M^2 - a^2}$, $r_- = M - \sqrt{M^2 - a^2}$, and δV denotes the deviation from the Regge-Wheeler potential. At the first order of $\sqrt{r_-/r_H} \simeq a/(2M)$, the deviation δV is given by

$$\delta V = \frac{f}{r_H^2}\sum_{j=0}^{5}\alpha_j\left(\frac{r_H}{r}\right)^j, \tag{57}$$

where the coefficients α_j are given by

$$\alpha_0 = -2m\omega_{\rm Sch}r_H\sqrt{\frac{r_-}{r_H}}, \tag{58}$$

$$\alpha_1 = -2m\omega_{\rm Sch}r_H\sqrt{\frac{r_-}{r_H}}, \tag{59}$$

$$\alpha_2 = m\omega_{\rm Sch}r_H\left(-2 - \frac{8}{\ell(\ell+1)}\right)\sqrt{\frac{r_-}{r_H}}, \tag{60}$$

$$\alpha_3 = \frac{8m(3 + 2(\ell^2 + \ell - 2))}{3\omega_{\rm Sch}r_H}\sqrt{\frac{r_-}{r_H}}, \tag{61}$$

$$\alpha_4 = -\frac{4m(5 + 2(\ell^2 + \ell - 2))}{\omega_{\rm Sch}r_H}\sqrt{\frac{r_-}{r_H}}, \tag{62}$$

$$\alpha_5 = \frac{12m}{\omega_{\rm Sch}r_H}\sqrt{\frac{r_-}{r_H}}. \tag{63}$$

Hence, the QNM frequency for a slowly rotating Kerr black hole is given by

$$\begin{aligned}\omega = \omega_{\rm Kerr}^{\rm 1st} &= \omega_{\rm Sch} + \frac{m}{r_H}\sqrt{\frac{r_-}{r_H}} + \sum_{j=0}^{5}\alpha_j e_j \\ &= \frac{\Omega_{\rm Sch}}{M} + \left[\frac{1}{4} - 2M\Omega_{\rm Sch}e_0 - 2M\Omega_{\rm Sch}e_1\right. \\ &\quad - \left(2 + \frac{8}{\ell + \ell^2}\right)M\Omega_{\rm Sch}e_2 + \frac{-2 + 4\ell(\ell+1)}{3\Omega_{\rm Sch}}Me_3 \\ &\quad \left. - \frac{1 + 2\ell(\ell+1)}{\Omega_{\rm Sch}}Me_4 + \frac{3Me_5}{\Omega_{\rm Sch}}\right]\frac{ma}{M^2} + \mathcal{O}(a^2).\end{aligned} \tag{64}$$

In Fig. 1 we plot the quasinormal frequencies for our first-order formula (64) and the numerical result in [107,108]. In Fig. 2 we plot the error functions defined by

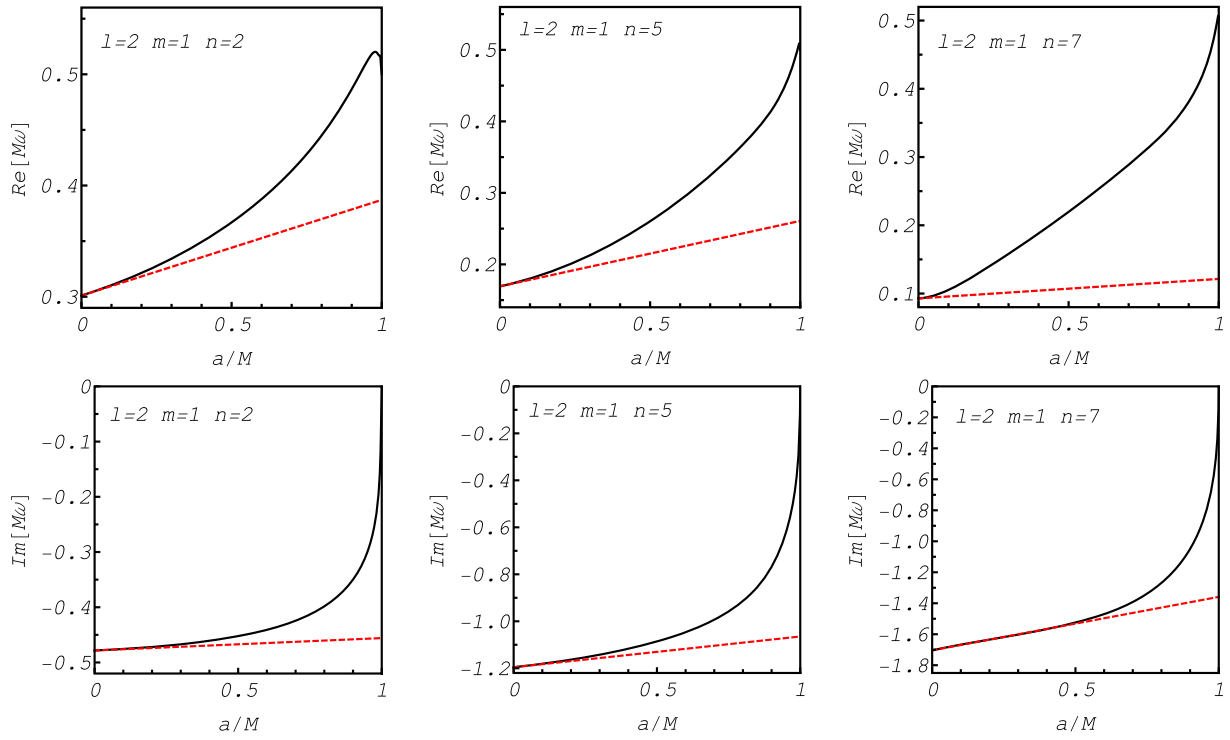

FIG. 1. Comparison with numerical calculation and our formula. Black lines denote the numerical result in [107,108] and red dashed lines denote our formula for slowly rotating Kerr black holes (64). We plot cases for $\ell = 2$, $m = 1$ and overtone numbers $n = 2$, 5, 7.

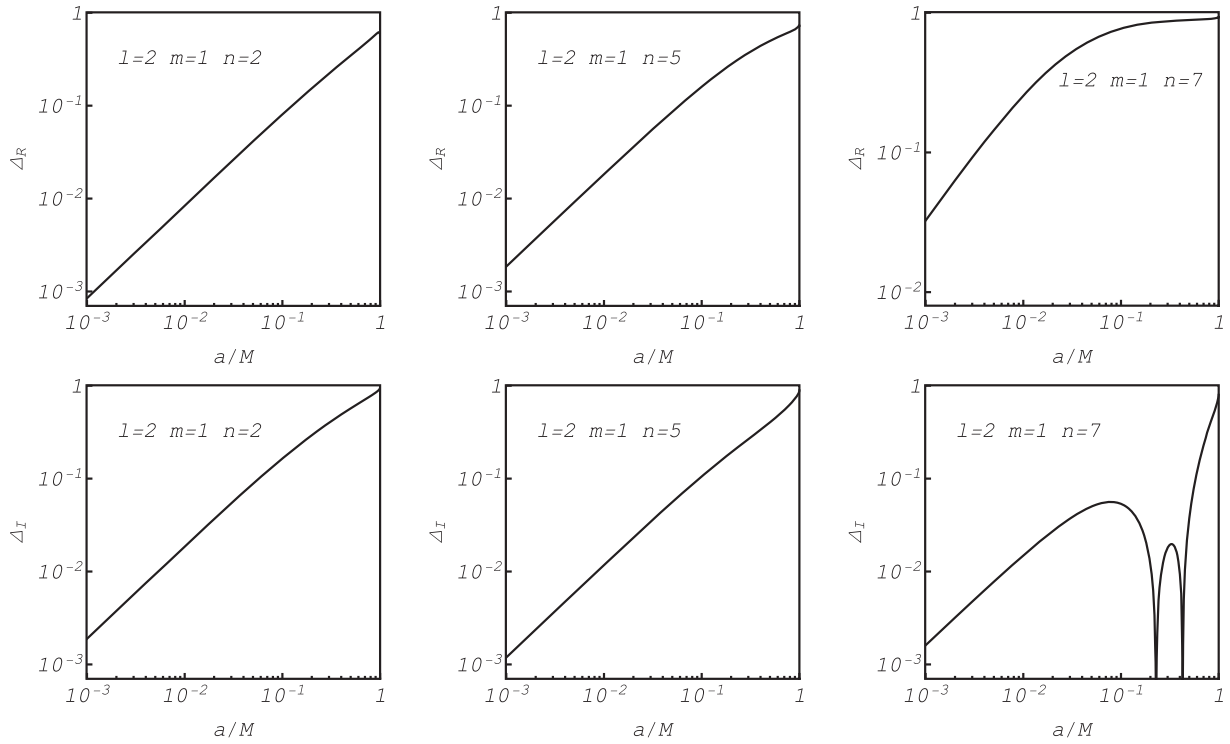

FIG. 2. Analysis of error functions in Eqs. (65) and (66) corresponding to modes with $\ell = 2$, $m = 1$, and overtone numbers $n = 2$, 5, 7.

$$\Delta_R = \left| \frac{\mathrm{Re}[(\omega_{\mathrm{full}} - \omega_{\mathrm{Sch}}) - (\omega^{\mathrm{1st}}_{\mathrm{Kerr}} - \omega_{\mathrm{Sch}})]}{\mathrm{Re}[\omega_{\mathrm{full}} - \omega_{\mathrm{Sch}}]} \right|, \quad (65)$$

$$\Delta_I = \left| \frac{\mathrm{Im}[(\omega_{\mathrm{full}} - \omega_{\mathrm{Sch}}) - (\omega^{\mathrm{1st}}_{\mathrm{Kerr}} - \omega_{\mathrm{Sch}})]}{\mathrm{Im}[\omega_{\mathrm{full}} - \omega_{\mathrm{Sch}}]} \right|, \quad (66)$$

where ω_{full} denotes the numerical result in [107,108] and $\omega^{\mathrm{1st}}_{\mathrm{Kerr}}$ denotes our first-order formula (64). Across various overtones, the imaginary part of the expression functions satisfactorily; however, the real part increasingly departs from numerical calculations as the overtone number n rises.

VI. SUMMARY AND DISCUSSION

In this paper, we studied the parametrized QNM formalism, with particular attention given to overtones. In this formalism, minor modifications to the GR-case effective potential are expressed in series expansion forms and they modify QNM behaviors at linear order in the deviations from GR. We adopted Nollert's method, known for its improved control over the larger imaginary parts, to numerically compute the precise values of the coefficients e_j. From the results, we observed that, in contrast to the fundamental mode, there exists a growing trend in the coefficients e_j as j increases and this trend is more evident as the overtone number n goes up. This suggests that the correction to the QNM frequency contributes significantly to overtones at large j. In typical modified gravity theories with higher-curvature correction terms, we confirmed that the deviation of the quasinormal frequencies from the GR value grows for higher overtones. Our findings indicate that if the overtones of QNMs are observed, they could be used to put a strong constraint on the gravity theories.

The growing tendency of e_j for overtones can also be understood using an analytical method. From the recursion relation for e_j in Eq. (A1), we derived the large-j asymptotic behavior as $e_j \simeq C j^{-1-2r_H\omega_I} e^{2ir_H\omega_R \ln j}$, where $\omega_{\mathrm{Sch}} = \omega_R + i\omega_I$. This implies that the magnitude of e_j is characterized by the factor $j^{-1-2r_H\omega_I}$. We confirmed that the power $-1-2r_H\omega_I$ becomes positive for overtones where ω_I has negative larger values than the fundamental mode. This is the essential reason why the magnitude of e_j for higher overtones grows as j increases. Also, since δV_j in Eq. (4) has a peak near the horizon $r_* = -r_H \ln(j/e)$ for large j, the increasing trend of the coefficient e_j for large j implies that modifications to the effective potential in the near-horizon regime strongly influence the overtones of QNMs, which is consistent with the recent discussion in [67]. Our result also helps us to understand recently confirmed findings that the overtone spectra are relatively more unstable against perturbations in the effective potential when compared to the fundamental mode [63–66]. Since higher-curvature modified gravity theories typically have modification terms with large j in the effective potential as discussed in Sec. V, the spectral instability of overtones is realized as the growing trend of quasinormal frequencies for overtones in such gravity theories. Our results are another physically important example of the QNM spectral instability [111].

Finally, we comment on the caveats of the extraction of the overtones from ringdown data. Considering the rapidly decaying nature of the overtones, their extractions are expected to be performed at the early ringdown phase with great care. The competing effects of nonlinear and linear gravitational perturbations should also be taken into account as the contribution of nonlinearity to the early ringdown phase may be significant. Many recent studies have tackled linear [12,15–17,21–23,31–39] and nonlinear analysis [25,29,30,112–133]. At the same time, we need to care about the determination of the starting time for the ringdown phase and the possibility of overfitting [27,28,40]. Toward the detection of overtones in real gravitational-wave data, we need an enhanced approach to the aforementioned issues in addition to the detector sensitivity.

ACKNOWLEDGMENTS

We would like to thank Emanuele Berti, Yasuyuki Hatsuda, and Hiroyuki Nakano for useful comments and discussions. This research is supported by JSPS KAKENHI Grants No. JP22K03626 (M. K.) and No. JP21H01080 (M. Y.), and IBS under the project code IBS-R018-D3 (M. Y. and J. Z.).

APPENDIX A: RECURSION RELATIONS AMONG THE COEFFICIENTS e_j

When analyzing parametrized QNMs, one can uncover a recursion relation [78,80] between the coefficients e_j with different subscripts j. This relation demonstrates the correlation between consecutive terms in the expansion. For the odd-parity case that we study, it is defined as follows:

$$c_{j+1}e_{j+1} + c_{j+3}e_{j+3} + c_{j+4}e_{j+4} + c_{j+5}e_{j+5} = 0, \quad (A1)$$

where the explicit form of c_{j+a} can be expressed as

$$c_{j+1} = -4jr_H^2(\omega_{\mathrm{Sch}})^2, \quad (A2)$$

$$c_{j+3} = -(\ell(\ell+1) - j(j+2)), \quad (A3)$$

$$c_{j+4} = (2j+3)(-6 - 2\ell(\ell+1) + j(j+3)), \quad (A4)$$

$$c_{j+5} = -(j-2)(j+2)(j+6). \quad (A5)$$

Such recursive structures are a result of perturbative methods applied to the gravitational equations governing the dynamics of the system under study as well as

underlying symmetries. The determination of the coefficients e_j for the parametrized QNM formalism can only be done manually, as the underlying equations are excessively complex. The identified recursive relations provide a notable computational benefit, enabling the estimation of coefficients for higher j via only the numerically computed values of e_j terms for lower j.

APPENDIX B: NONTRIVIAL RELATION INCLUDING e_1

It should be noted that the recursion relation described in the previous appendix does not include the relation between the coefficient e_1 and the other components. Nevertheless, this nontrivial connection can be obtained using the following strategy.

In [134], the equation

$$\left(1-\frac{r_H}{r}\right)\frac{d}{dr}\left(\left(1-\frac{r_H}{r}\right)\frac{d\tilde{\Phi}}{dr}\right)+((2M\omega)^2-\tilde{V})\tilde{\Phi}=0, \tag{B1}$$

with

$$\tilde{V}=\left(1-\frac{r_H}{r}\right)\left(\frac{4a^2\omega^2}{r_H^2}+\frac{4a\omega(m-a\omega)}{r_H r}+\frac{A_{\ell,m}+2-a\omega(2m-a\omega)}{r^2}-\frac{3r_H}{r^3}\right), \tag{B2}$$

was proposed as an isospectral equation to the radial spin-2 Teukolsky equation [7]. Taking the slow-rotation limit, we can rewrite the potential as

$$\tilde{V}=\left(1-\frac{r_H}{r}\right)\left(\frac{\ell(\ell+1)}{r^2}-\frac{3r_H}{r^3}+\frac{\tilde{\alpha}_1}{r_H^2}\left(\frac{r_H}{r}\right)+\frac{\tilde{\alpha}_2}{r_H^2}\left(\frac{r_H}{r}\right)^2+\mathcal{O}(a^2)\right), \tag{B3}$$

with

$$\tilde{\alpha}_1=4mr_H\omega_{\rm Sch}\sqrt{\frac{r_-}{r_H}}, \tag{B4}$$

$$\tilde{\alpha}_2=-2\left(1+\frac{4}{\ell+\ell^2}\right)mr_H\omega_{\rm Sch}\sqrt{\frac{r_-}{r_H}}. \tag{B5}$$

Using the parametrized QNM formalism, we obtain the QNM frequency for a slowly rotating Kerr black hole as

$$\omega=\omega_{\rm Sch}+\tilde{\alpha}_1 e_1+\tilde{\alpha}_1 e_2. \tag{B6}$$

Comparing this formula to Eq. (64), we obtain a nontrivial relation that contains e_1 as

$$-3\omega_{\rm Sch}+6r_H^2\omega_{\rm Sch}^2 e_0+18r_H^2\omega_{\rm Sch}^2 e_1-8(-1+2\ell+2\ell^2)e_3+12(1+2\ell+2\ell^2)e_4-36e_5=0. \tag{B7}$$

Using Eq. (A1), this relation can be rewritten in the simpler form

$$-6\omega_{\rm Sch}+36r_H^2\omega_{\rm Sch}^2 e_1-2(-20+7\ell+7\ell^2)e_3+15(-5+2\ell+2\ell^2)e_4=0. \tag{B8}$$

APPENDIX C: COEFFICIENTS e_j FOR $n=8$, $\ell=2$ OVERTONE

In the Schwarzschild limit, there are special solutions where the series in Eq. (9) becomes a finite series, making $\sum_{k=0}^{\infty}a_k$ clearly convergent. Specifically, for the $\ell=2$ case, the frequency for such a solution is given by $\omega=-4i/r_H$ and the wave function becomes

$$\Phi_{\rm Sch}^{n=8}=C\exp(i\omega r_*)f^{\rho}\left(-\frac{945}{4194304}+\frac{15525f}{4194304}-\frac{29025f^2}{1048576}+\frac{130185f^3}{1048576}-\frac{775935f^4}{2097152}+\frac{1604979f^5}{2097152}-\frac{1164765f^6}{1048576}+\frac{1164765f^7}{1048576}-\frac{2717785f^8}{4194304}+\frac{1164765f^9}{4194304}\right), \tag{C1}$$

with $\rho=-2ir_H\omega$. This solution is known as the algebraically special mode [62] and the frequency $\omega=-4i/r_H$ corresponds to the $n=8$ overtone for the $\ell=2$ Schwarzschild case. However, we should note that according to [135] there exists an argument that for such a special frequency the QNM boundary condition fails to hold at the horizon. Nevertheless, in this appendix we discuss the shift of frequency of the $n=8$ mode for the parametrized potential in Eq. (4).

To discuss the coefficient e_j in Eq (7) for the $n=8$, $\ell=2$ overtone, we assume the same form of the wave function Φ in Eq. (9) with $\rho=-2ir_H\omega$, whose GR limit is given by Eq. (C1). For the parametrized potential in Eq. (4), we obtain a recursion relation for a_j. After analyzing this recursion relation, we find the frequency in the form

$$\omega=-\frac{4i}{r_H}+\sum_j\alpha_j e_j, \tag{C2}$$

and the coefficients e_j are given by

$$r_H e_0 = \frac{1164765i}{700009}, \tag{C3}$$

$$r_H e_1 = \frac{5571603i}{1400018}, \tag{C4}$$

$$r_H e_2 = \frac{5823825i}{700009}, \tag{C5}$$

$$r_H e_3 = \frac{44416947i}{2800036}, \tag{C6}$$

$$r_H e_4 = \frac{19775313i}{700009}, \tag{C7}$$

$$r_H e_5 = \frac{66780435i}{1400018}, \tag{C8}$$

$$r_H e_6 = \frac{3176547i}{41177}, \tag{C9}$$

$$r_H e_7 = \frac{674140005i}{5600072}. \tag{C10}$$

Note that these coefficients e_j satisfy the relation in Eq. (A1), and e_j with $j \geq 8$ can be generated from Eq. (A1).

Substituting the above coefficients e_j into the formula for a slowly rotating Kerr black hole in Eq. (64), we obtain

$$2M\omega = -4i - \frac{33078176}{700009}\frac{ma}{2M} + \mathcal{O}(a^2). \tag{C11}$$

This completely coincides with the result at the order $\mathcal{O}(a)$ in [135–137]. References [138,139] reported that QNM frequencies for slowly rotating Kerr black holes calculated numerically agree with the prediction (C11) for branches where $2M\omega \to -4i$ in the $a \to 0$ limit.

APPENDIX D: DIMENSIONLESS SCHWARZSCHILD QUASINORMAL FREQUENCIES Ω_{Sch}

We provide numerical values of Ω_{Sch}, which are dimensionless quasinormal frequencies normalized by the mass (not the black hole radius) for the Schwarzschild black holes in Tables VI and VII, where n denotes the overtone number.

TABLE VI. $\ell = 2$ Schwarzschild QNM frequencies normalized by the mass.

n	Ω_{Sch} for $\ell = 2$
0	$0.37367168441804183579349200 2977 - 0.08896231568893569828046092 7185i$
1	$0.34671099687916343971767535 9733 - 0.27391487529123481734956022 2138i$
2	$0.30105345461236639380200360 8880 - 0.47827698322307180998418283 0723i$
3	$0.25150496218559058945554044 7872 - 0.70514820243349536858619705 0439i$
4	$0.20751457981306557953306867 9253 - 0.94684489086635154728536211 7782i$
5	$0.16929940309304366054380646 9280 - 1.19560805413584680784746002 9672i$
6	$0.13325234024518802334878268 918 - 1.44791062616203815799480739 742i$
7	$0.09282233367020094511758196 991 - 1.70384117220613552700100693 606i$
8	$-2i$
9	$0.06326350512560599307041854 974 - 2.30264476515854049612775361 250i$
10	$0.07655346288598616222699244 005 - 2.56082661738150570057182167 367i$

TABLE VII. $\ell = 3$ Schwarzschild QNM frequencies normalized by the mass.

n	Ω_{Sch} for $\ell = 3$
0	$0.59944328843749007273949397 7601 - 0.09270304794494760397000741 06711i$
1	$0.58264380303329943061584078 5500 - 0.28129811343504404467883826 4497i$
2	$0.55168490077845131638641178 9182 - 0.47909275096696223496818754 5681i$
3	$0.51196191105833738211925660 1539 - 0.69033709596923910651136606 5005i$
4	$0.47017400581515522814342747 8927 - 0.91564939250509660663710636 3461i$
5	$0.43138647864215384492216714 4935 - 1.15215136214090543899531299 4801i$
6	$0.39765952417575710857715463 748 - 1.39591224272259156879382199 256i$
7	$0.36899227588972845769529171 517 - 1.64384452835676619241220936 938i$
8	$0.34461831859511639569908026 946 - 1.89403280419296282019417602 374i$
9	$0.32368313160134644137286356 638 - 2.14539894976732050705523618 001i$
10	$0.30546090193109574672725993 056 - 2.39735455030161310920191229 124i$

APPENDIX E: NUMERICAL DATA FOR e_j

We provide numerical values of the coefficients e_j in the parametrized QNM formalism for $\ell = 2, 3$ and $n = 0, 1, \ldots 10$ in Tables VIII–XVIII, where the values are normalized by the horizon radius r_H. We note that the coefficients e_j with high j can be generated from the recursion relation (A1).

TABLE VIII. e_j data for $n = 0$.

		$\ell = 2$
ℓ	j	$r_H e_j$
	0	$0.247251965436735 + 0.092643073755839i$
	1	$0.159854787039703 + 0.018208481773442i$
	2	$0.0966322401342324 - 0.0024154964534615i$
	3	$0.0584907850084892 - 0.0037178612876936i$
	4	$0.0366794367818616 - 0.0004386969534051i$
2	5	$0.0240379477506994 + 0.0027307931425322i$
	6	$0.0163428109579658 + 0.0048426716837515i$
	7	$0.01136357508132363 + 0.00601399193209594i$
	8	$0.00795199773524588 + 0.00653699645743769i$
	9	$0.00550386682041598 + 0.00665277086108331i$
	10	$0.00368531438581036 + 0.00652444451724573i$
		$\ell = 3$
ℓ	j	$r_H e_j$
	0	$0.144427428250107 + 0.036770321741985i$
	1	$0.0957683223248566 + 0.0086035480579422i$
	2	$0.0614725008272383 - 0.0006195234760257i$
	3	$0.0392928459198075 - 0.0020278784624223i$
	4	$0.0254322953286445 - 0.0009608457364406i$
3	5	$0.0167854156428019 + 0.0004525854131922i$
	6	$0.01128895497550895 + 0.00154867984591634i$
	7	$0.00769038142142765 + 0.00222885207817423i$
	8	$0.00525650581974478 + 0.00256801534497293i$
	9	$0.00355997381645353 + 0.00266834227449026i$
	10	$0.00234751849358300 + 0.00261518583054406i$

TABLE IX. e_j data for $n = 1$.

		$\ell = 2$
ℓ	j	$r_H e_j$
	0	$0.107464723514924 + 0.185387391385682i$
	1	$0.146179872594831 + 0.052434921070417i$
	2	$0.1041379948373251 - 0.0044390476970642i$
	3	$0.0652386112046042 - 0.0101870692777796i$
	4	$0.0442462688718310 - 0.0007443024387448i$
2	5	$0.0343154937570156 + 0.0085123887906039i$
	6	$0.0288347045024162 + 0.0146400895953562i$
	7	$0.0247495202489046 + 0.0183738440993958i$
	8	$0.0210862837711776 + 0.0207122863689407i$
	9	$0.0176399327840039 + 0.0222573314442506i$
	10	$0.0144010839340230 + 0.0233065697436193i$
		$\ell = 3$
ℓ	j	$r_H e_j$
	0	$0.1006072239125757 + 0.0915010162162569i$
	1	$0.0908230933313796 + 0.0251617955322758i$
	2	$0.0631457098839271 - 0.0012762849371758i$
	3	$0.0405826063112734 - 0.0058654477129917i$
	4	$0.0266444759092582 - 0.0027460041524308i$
3	5	$0.0187515720371715 + 0.0014333798543680i$
	6	$0.0140972716344782 + 0.0046182669826315i$
	7	$0.01097558821497615 + 0.00661974226141833i$
	8	$0.00857150329016809 + 0.00773824127797637i$
	9	$0.00654988811306071 + 0.00828024569376265i$
	10	$0.00478503575349286 + 0.00845673795231441i$

TABLE X. e_j data for $n = 2$.

$\ell = 2$		
ℓ	j	$r_H e_j$
	0	$-0.006678041383435 + 0.1414600347512 57i$
	1	$0.1193062609510017 + 0.0756163764534419i$
	2	$0.1146657081287942 + 0.0007488463687182i$
	3	$0.0782877891066255 - 0.0131338321833861i$
	4	$0.0599473129083836 + 0.0012772989022803i$
2	5	$0.0565936649372375 + 0.0160077547135168i$
	6	$0.0568488399946155 + 0.0255671324891611i$
	7	$0.0560425975806698 + 0.0325413833400877i$
	8	$0.0539183634932275 + 0.0390560260774349i$
	9	$0.0511353840916677 + 0.0456725141154477i$
	10	$0.0480745969771377 + 0.0522805954645665i$

$\ell = 3$		
ℓ	j	$r_H e_j$
	0	$0.0417297228847025 + 0.1054357814502190i$
	1	$0.0809446392217919 + 0.0393002156329161i$
	2	$0.0657815259440879 - 0.0003182440479682i$
	3	$0.0430191259862773 - 0.0089970325320210i$
	4	$0.0289927226551848 - 0.0040793839493983i$
3	5	$0.0226844579843885 + 0.0026963752537984i$
	6	$0.0197951387879185 + 0.0076629122566710i$
	7	$0.0177112285288053 + 0.0108680547155301i$
	8	$0.0155449354304499 + 0.0130679060054845i$
	9	$0.0131958602719892 + 0.0147600683337322i$
	10	$0.0107593575889026 + 0.0161444044960749i$

TABLE XI. e_j data for $n = 3$.

$\ell = 2$		
ℓ	j	$r_H e_j$
	0	$-0.0325852551314068 + 0.0747719102635759i$
	1	$0.0913442595092874 + 0.0802769838946251i$
	2	$0.1221777342069701 + 0.0103635649576794i$
	3	$0.0956292086910920 - 0.0116599781393095i$
	4	$0.0841321049646752 + 0.0067377139623656i$
2	5	$0.0936680274794272 + 0.0268198345546321i$
	6	$0.1063650780631990 + 0.0394793789659170i$
	7	$0.1150476659540682 + 0.0513105036772837i$
	8	$0.1214885885651855 + 0.0665332576927772i$
	9	$0.127970980521597 + 0.084915740662278i$
	10	$0.134865872349529 + 0.105123598889745i$

$\ell = 3$		
ℓ	j	$r_H e_j$
	0	$-0.0015779165948527 + 0.0873367275805243i$
	1	$0.0673743381165955 + 0.0486885005868322i$
	2	$0.0679844063269548 + 0.0025796969637562i$
	3	$0.0461217486198088 - 0.0109948921592254i$
	4	$0.0321822975816820 - 0.0046665357787451i$
3	5	$0.0284401186916899 + 0.0044902751481566i$
	6	$0.0284145137326224 + 0.0107615638124564i$
	7	$0.0281106342904294 + 0.0149900036743692i$
	8	$0.0267641215905967 + 0.0187884225796811i$
	9	$0.0247640461065528 + 0.0227806369056446i$
	10	$0.0224497106473862 + 0.0269194971851201i$

TABLE XII. e_j data for $n = 4$.

ℓ	j	$r_H e_j$
		$\ell = 2$
	0	$-0.0231849383760028 + 0.0386350792467110i$
	1	$0.0745603838858844 + 0.0739685626200772i$
	2	$0.1289818292501889 + 0.0185747235596811i$
	3	$0.1185869296093861 - 0.0075521097199608i$
	4	$0.1208149855689374 + 0.0153836167032158i$
2	5	$0.153246787920723 + 0.042165247302196i$
	6	$0.190883591791763 + 0.059087655770938i$
	7	$0.223122109713004 + 0.079607772795008i$
	8	$0.256242481590652 + 0.111916146131414i$
	9	$0.295805911965927 + 0.153900293946673i$
	10	$0.341401447538711 + 0.202009507605051i$
		$\ell = 3$
	0	$-0.0206699647600537 + 0.0604937732682900i$
	1	$0.0531273798618641 + 0.0521831825708380i$
	2	$0.0685467879135409 + 0.0065104733363981i$
	3	$0.0491845253435823 - 0.0118840345930306i$
	4	$0.0357563149149284 - 0.0045009772316074i$
3	5	$0.0357171302438170 + 0.0068894045675336i$
	6	$0.0398939005969786 + 0.0139081057618229i$
	7	$0.0423766399766888 + 0.0189679808169785i$
	8	$0.0429977895228710 + 0.0251497406761657i$
	9	$0.0430899787206310 + 0.0330274154954972i$
	10	$0.0431505747879606 + 0.0419485811820150i$

TABLE XIII. e_j data for $n = 5$.

ℓ	j	$r_H e_j$
		$\ell = 2$
	0	$-0.0094305225379713 + 0.0228491067858833i$
	1	$0.0702008814396801 + 0.0662882049778363i$
	2	$0.142252676129377 + 0.025405358939820i$
	3	$0.154620812604551 - 0.000423219329531i$
	4	$0.182203230561820 + 0.029504645326924i$
2	5	$0.255336456159544 + 0.066808671315109i$
	6	$0.342726500675614 + 0.092694584974768i$
	7	$0.430371143569840 + 0.130949071521098i$
	8	$0.533689309697611 + 0.196920669397476i$
	9	$0.665552920988299 + 0.285553231284859i$
	10	$0.824806651834691 + 0.390298807833414i$
		$\ell = 3$
	0	$-0.0242359941938532 + 0.0391998561347797i$
	1	$0.0410525578207275 + 0.0510883587925916i$
	2	$0.0674611376093846 + 0.0101191863850904i$
	3	$0.0518041022306143 - 0.0121462820686405i$
	4	$0.0394451464476780 - 0.0038860226006234i$
3	5	$0.0443110947175641 + 0.0097199793849433i$
	6	$0.0542554531049167 + 0.0169330906459240i$
	7	$0.0608334954196972 + 0.0226710726902531i$
	8	$0.0652918023688233 + 0.0323530592228630i$
	9	$0.0706834627858642 + 0.0461483209546148i$
	10	$0.0774416624771747 + 0.0622664396956380i$

TABLE XIV. e_j data for $n = 6$.

$\ell = 2$		
ℓ	j	$r_H e_j$
	0	$0.0071189800022886 + 0.0244270829307704i$
	1	$0.0791909802110347 + 0.0620357577486420i$
	2	$0.173115614615052 + 0.035388200761421i$
	3	$0.222901483433564 + 0.015778312404325i$
	4	$0.301561328505558 + 0.059893181498572i$
2	5	$0.455611505703941 + 0.118981345967461i$
	6	$0.651812379158736 + 0.169875613740407i$
	7	$0.876783760510318 + 0.251723052069271i$
	8	$1.165440235050287 + 0.392822370971920i$
	9	$1.54894032266647 + 0.58575879231756i$
	10	$2.03128586446286 + 0.82238818017992i$

$\ell = 3$		
ℓ	j	$r_H e_j$
	0	$-0.0218337427685166 + 0.0255734369366163i$
	1	$0.0320875572902621 + 0.0477002188031165i$
	2	$0.0655086920252467 + 0.0127396297373017i$
	3	$0.0540292854986211 - 0.0122365023143462i$
	4	$0.0432800997782630 - 0.0031200844577528i$
3	5	$0.0542418031712442 + 0.0127726879121193i$
	6	$0.0717092006682787 + 0.0196507330512797i$
	7	$0.0840206147652311 + 0.0259611517154740i$
	8	$0.0950486968143402 + 0.0406293154981293i$
	9	$0.1108277658771737 + 0.0628258921132427i$
	10	$0.131373960775933 + 0.088831277287416i$

TABLE XV. e_j data for $n = 7$.

$\ell = 2$		
ℓ	j	$r_H e_j$
	0	$0.0287995454850320 + 0.0184008711381451i$
	1	$0.1185260892634616 + 0.0702388413679524i$
	2	$0.262798164747494 + 0.067651801946992i$
	3	$0.402418479961720 + 0.075446166908563i$
	4	$0.619265957172561 + 0.167123015914277i$
2	5	$0.990929923676543 + 0.300580618898559i$
	6	$1.50132244234922 + 0.45516305413662i$
	7	$2.16022900341441 + 0.69861773253752i$
	8	$3.05660702313977 + 1.08904787182772i$
	9	$4.28089213354471 + 1.62947163418331i$
	10	$5.88191594348812 + 2.32700575812425i$

$\ell = 3$		
ℓ	j	$r_H e_j$
	0	$-0.0181695599769233 + 0.0173653805837275i$
	1	$0.0258006211401533 + 0.0436621925138659i$
	2	$0.0633760140904404 + 0.0144010604651561i$
	3	$0.0560671363333610 - 0.0123560243951517i$
	4	$0.0474063165779652 - 0.0023395700887393i$
3	5	$0.0656394145006476 + 0.0159386609575311i$
	6	$0.0925735912492434 + 0.0219612321451617i$
	7	$0.1126404955138170 + 0.0287748178212681i$
	8	$0.133997197586964 + 0.050300439609534i$
	9	$0.167594131545889 + 0.083835192044083i$
	10	$0.212604721378107 + 0.122574246944150i$

TABLE XVI. e_j data for $n = 8$.

$\ell = 2$			
	ℓ	j	$r_H e_j$
		0	$1164765i/700009$
		1	$5571603i/1400018$
		2	$5823825i/700009$
		3	$44416947i/2800036$
		4	$19775313i/700009$
	2	5	$66780435i/1400018$
		6	$3176547i/41177$
		7	$674140005i/5600072$
		8	$127575708i/700009$
		9	$188176863i/700009$
		10	$271337670i/700009$

$\ell = 3$		
ℓ	j	$r_H e_j$
	0	$-0.0147928320971783 + 0.0123743181062329i$
	1	$0.0214391560286977 + 0.0397521519745856i$
	2	$0.0614090924597511 + 0.0153637244331753i$
	3	$0.0580838091121277 - 0.0125425795554257i$
	4	$0.0519502219622454 - 0.0015730406072024i$
3	5	$0.0786457141341650 + 0.0191862568338425i$
	6	$0.1172032879552634 + 0.0238326931912907i$
	7	$0.147509636765554 + 0.031110164267112i$
	8	$0.184171013412476 + 0.061763756771027i$
	9	$0.245875062224800 + 0.110035571897353i$
	10	$0.330574124897447 + 0.164396535331579i$

TABLE XVII. e_j data for $n = 9$.

$\ell = 2$		
ℓ	j	$r_H e_j$
	0	$-0.0481759684369441 + 0.0198318150040291i$
	1	$-0.0857100274407277 + 0.0696760632695613i$
	2	$-0.163048616819628 + 0.088879078933767i$
	3	$-0.399175255262569 + 0.12223674006529i$
	4	$-0.81065760615737 + 0.260087843129221i$
2	5	$-1.42480435859151 + 0.46296090697546i$
	6	$-2.45012481988937 + 0.70044231531924i$
	7	$-4.13067788001983 + 1.09884440280146i$
	8	$-6.62226314194639 + 1.77828164952022i$
	9	$-10.16840189854991 + 2.71688284859888i$
	10	$-15.263695475771 + 3.8936799351803i$

$\ell = 3$		
ℓ	j	$r_H e_j$
	0	$-0.0120283376057713 + 0.0092268293347515i$
	1	$0.0183816535851371 + 0.0362400948763753i$
	2	$0.0597273795213759 + 0.0158699469639609i$
	3	$0.0601776636210653 - 0.0127784268842468i$
	4	$0.0570000117323253 - 0.0008112575506905i$
3	5	$0.0933947167540892 + 0.0225146379534043i$
	6	$0.145978216615856 + 0.025264285239297i$
	7	$0.189560074188723 + 0.032997533643411i$
	8	$0.247936809811029 + 0.075464851825739i$
	9	$0.351473842723456 + 0.142352794591404i$
	10	$0.496761868293284 + 0.215162791465753i$

TABLE XVIII. e_j data for $n = 10$.

$\ell = 2$		
ℓ	j	$r_H e_j$
	0	$-0.0286426058703113 + 0.0106113087976747i$
	1	$-0.0441254333176308 + 0.0464183237687842i$
	2	$-0.0752048505169943 + 0.0468937958675964i$
	3	$-0.227596261935816 + 0.042132374231758i$
	4	$-0.508076137978851 + 0.118357621671413i$
2	5	$-0.915575048516598 + 0.224172274528923i$
	6	$-1.64633503018129 + 0.29889860678943i$
	7	$-2.94384311234699 + 0.46714791896406i$
	8	$-4.91739505425679 + 0.85380608133462i$
	9	$-7.75386071925519 + 1.37454445656736i$
	10	$-11.97130226833821 + 1.91254938844106i$

$\ell = 3$		
ℓ	j	$r_H e_j$
	0	$-0.00983772607665567 + 0.00715383021451585i$
	1	$0.0162007321968787 + 0.0331738592666763i$
	2	$0.058347734545312 + 0.016090541198903i$
	3	$0.0624036576883143 - 0.0130377492445573i$
	4	$0.0626211364925363 - 0.0000384220075813i$
3	5	$0.1100219464703823 + 0.0259314159606847i$
	6	$0.17931606216785 + 0.026268228832864i$
	7	$0.239862602404814 + 0.034485599094529i$
	8	$0.328047625741178 + 0.091885300951663i$
	9	$0.491232700613689 + 0.181775433171764i$
	10	$0.725014956209716 + 0.275712379374871i$

[1] B. P. Abbott *et al.* (LIGO Scientific and Virgo Collaborations), Phys. Rev. Lett. **116**, 061102 (2016).
[2] B. P. Abbott *et al.* (LIGO Scientific and Virgo Collaborations), Phys. Rev. D **93**, 122003 (2016).
[3] W. Israel, Phys. Rev. **164**, 1776 (1967).
[4] B. Carter, Phys. Rev. Lett. **26**, 331 (1971).
[5] D. C. Robinson, Phys. Rev. Lett. **34**, 905 (1975).
[6] S. A. Teukolsky, Phys. Rev. Lett. **29**, 1114 (1972).
[7] S. A. Teukolsky, Astrophys. J. **185**, 635 (1973).
[8] W. H. Press and S. A. Teukolsky, Astrophys. J. **185**, 649 (1973).
[9] C. D. Capano and A. H. Nitz, Phys. Rev. D **102**, 124070 (2020).
[10] C. D. Capano, M. Cabero, J. Westerweck, J. Abedi, S. Kastha, A. H. Nitz, Y. F. Wang, A. B. Nielsen, and B. Krishnan, Phys. Rev. Lett. **131**, 221402 (2023).
[11] B. P. Abbott *et al.* (LIGO Scientific and Virgo Collaborations), Phys. Rev. Lett. **116**, 221101 (2016); **121**, 129902(E) (2018).
[12] M. Giesler, M. Isi, M. A. Scheel, and S. Teukolsky, Phys. Rev. X **9**, 041060 (2019).
[13] R. Cotesta, G. Carullo, E. Berti, and V. Cardoso, Phys. Rev. Lett. **129**, 111102 (2022).
[14] A. Correia, Y. F. Wang, J. Westerweck, and C. D. Capano, arXiv:2312.14118.
[15] G. B. Cook, Phys. Rev. D **102**, 024027 (2020).
[16] X. Jiménez Forteza, S. Bhagwat, P. Pani, and V. Ferrari, Phys. Rev. D **102**, 044053 (2020).
[17] P. Mourier, X. Jiménez Forteza, D. Pook-Kolb, B. Krishnan, and E. Schnetter, Phys. Rev. D **103**, 044054 (2021).
[18] N. Sago, S. Isoyama, and H. Nakano, Universe **7**, 357 (2021).
[19] M. Isi, W. M. Farr, M. Giesler, M. A. Scheel, and S. A. Teukolsky, Phys. Rev. Lett. **127**, 011103 (2021).
[20] N. Oshita, Phys. Rev. D **104**, 124032 (2021).
[21] X. J. Forteza and P. Mourier, Phys. Rev. D **104**, 124072 (2021).
[22] L. Magaña Zertuche, K. Mitman, N. Khera, L. C. Stein, M. Boyle, N. Deppe, F. Hébert, D. A. B. Iozzo, L. E. Kidder, J. Moxon *et al.*, Phys. Rev. D **105**, 104015 (2022).
[23] A. Dhani, Phys. Rev. D **103**, 104048 (2021).

[24] K. Takahashi and H. Motohashi, arXiv:2311.12762.
[25] M. H. Y. Cheung, E. Berti, V. Baibhav, and R. Cotesta, Phys. Rev. D **109**, 044069 (2024).
[26] H. Zhu, J. L. Ripley, A. Cárdenas-Avendaño, and F. Pretorius, Phys. Rev. D **109**, 044010 (2024).
[27] P. J. Nee, S. H. Völkel, and H. P. Pfeiffer, Phys. Rev. D **108**, 044032 (2023).
[28] V. Baibhav, M. H. Y. Cheung, E. Berti, V. Cardoso, G. Carullo, R. Cotesta, W. Del Pozzo, and F. Duque, Phys. Rev. D **108**, 104020 (2023).
[29] K. Mitman, M. Lagos, L. C. Stein, S. Ma, L. Hui, Y. Chen, N. Deppe, F. Hébert, L. E. Kidder, J. Moxon *et al.*, Phys. Rev. Lett. **130**, 081402 (2023).
[30] M. H. Y. Cheung, V. Baibhav, E. Berti, V. Cardoso, G. Carullo, R. Cotesta, W. Del Pozzo, F. Duque, T. Helfer, E. Shukla *et al.*, Phys. Rev. Lett. **130**, 081401 (2023).
[31] V. Baibhav, E. Berti, V. Cardoso, and G. Khanna, Phys. Rev. D **97**, 044048 (2018).
[32] L. London, D. Shoemaker, and J. Healy, Phys. Rev. D **90**, 124032 (2014); **94**, 069902(E) (2016).
[33] S. Bhagwat, X. J. Forteza, P. Pani, and V. Ferrari, Phys. Rev. D **101**, 044033 (2020).
[34] J. Calderón Bustillo, P. D. Lasky, and E. Thrane, Phys. Rev. D **103**, 024041 (2021).
[35] A. Dhani and B. S. Sathyaprakash, arXiv:2107.14195.
[36] E. Finch and C. J. Moore, Phys. Rev. D **103**, 084048 (2021).
[37] E. Finch and C. J. Moore, Phys. Rev. D **104**, 123034 (2021).
[38] I. Ota and C. Chirenti, Phys. Rev. D **101**, 104005 (2020).
[39] I. Ota and C. Chirenti, Phys. Rev. D **105**, 044015 (2022).
[40] N. Franchini and S. H. Völkel, arXiv:2305.01696.
[41] B. P. Abbott *et al.* (LIGO Scientific and Virgo Collaborations), Phys. Rev. D **100**, 104036 (2019).
[42] R. Abbott *et al.* (LIGO Scientific and Virgo Collaborations), Phys. Rev. D **103**, 122002 (2021).
[43] R. Abbott *et al.* (LIGO Scientific, Virgo, and KAGRA Collaborations), arXiv:2112.06861.
[44] A. Ghosh, R. Brito, and A. Buonanno, Phys. Rev. D **103**, 124041 (2021).
[45] M. Isi, M. Giesler, W. M. Farr, M. A. Scheel, and S. A. Teukolsky, Phys. Rev. Lett. **123**, 111102 (2019).
[46] M. Isi and W. M. Farr, arXiv:2202.02941.
[47] M. Isi and W. M. Farr, Phys. Rev. Lett. **131**, 169001 (2023).
[48] G. Carullo, R. Cotesta, E. Berti, and V. Cardoso, Phys. Rev. Lett. **131**, 169002 (2023).
[49] E. Finch and C. J. Moore, Phys. Rev. D **106**, 043005 (2022).
[50] H. T. Wang and L. Shao, Phys. Rev. D **108**, 123018 (2023).
[51] Y. F. Wang, C. D. Capano, J. Abedi, S. Kastha, B. Krishnan, A. B. Nielsen, A. H. Nitz, and J. Westerweck, arXiv:2310.19645.
[52] L. Barack, V. Cardoso, S. Nissanke, T. P. Sotiriou, A. Askar, C. Belczynski, G. Bertone, E. Bon, D. Blas, R. Brito *et al.*, Classical Quantum Gravity **36**, 143001 (2019).
[53] E. Berti, E. Barausse, V. Cardoso, L. Gualtieri, P. Pani, U. Sperhake, L. C. Stein, N. Wex, K. Yagi, T. Baker *et al.*, Classical Quantum Gravity **32**, 243001 (2015).
[54] E. Berti, V. Cardoso, and C. M. Will, Phys. Rev. D **73**, 064030 (2006).
[55] J. Meidam, M. Agathos, C. Van Den Broeck, J. Veitch, and B. S. Sathyaprakash, Phys. Rev. D **90**, 064009 (2014).
[56] E. Berti, A. Sesana, E. Barausse, V. Cardoso, and K. Belczynski, Phys. Rev. Lett. **117**, 101102 (2016).
[57] E. Berti, K. Yagi, H. Yang, and N. Yunes, Gen. Relativ. Gravit. **50**, 49 (2018).
[58] V. Cardoso, M. Kimura, A. Maselli, E. Berti, C. F. B. Macedo, and R. McManus, Phys. Rev. D **99**, 104077 (2019).
[59] Y. Hatsuda and M. Kimura, Phys. Rev. D **102**, 044032 (2020).
[60] H. P. Nollert, Phys. Rev. D **47**, 5253 (1993).
[61] S. H. Völkel, N. Franchini, and E. Barausse, Phys. Rev. D **105**, 084046 (2022).
[62] S. Chandrasekhar, Proc. R. Soc. A **392**, 1 (1984).
[63] J. L. Jaramillo, R. Panosso Macedo, and L. Al Sheikh, Phys. Rev. X **11**, 031003 (2021).
[64] J. L. Jaramillo, R. Panosso Macedo, and L. A. Sheikh, Phys. Rev. Lett. **128**, 211102 (2022).
[65] M. H. Y. Cheung, K. Destounis, R. P. Macedo, E. Berti, and V. Cardoso, Phys. Rev. Lett. **128**, 111103 (2022).
[66] E. Berti, V. Cardoso, M. H. Y. Cheung, F. Di Filippo, F. Duque, P. Martens, and S. Mukohyama, Phys. Rev. D **106**, 084011 (2022).
[67] R. A. Konoplya and A. Zhidenko, arXiv:2209.00679.
[68] T. Regge and J. A. Wheeler, Phys. Rev. **108**, 1063 (1957).
[69] R. McManus, E. Berti, C. F. B. Macedo, M. Kimura, A. Maselli, and V. Cardoso, Phys. Rev. D **100**, 044061 (2019).
[70] O. J. Tattersall, Classical Quantum Gravity **37**, 115007 (2020).
[71] C. de Rham, J. Francfort, and J. Zhang, Phys. Rev. D **102**, 024079 (2020).
[72] S. H. Völkel, N. Franchini, E. Barausse, and E. Berti, Phys. Rev. D **106**, 124036 (2022).
[73] N. Franchini and S. H. Völkel, Phys. Rev. D **107**, 124063 (2023).
[74] S. S. Lahoz and J. Noller, Phys. Rev. D **107**, 124054 (2023).
[75] S. Mukohyama, K. Takahashi, K. Tomikawa, and V. Yingcharoenrat, J. Cosmol. Astropart. Phys. 07 (2023) 050.
[76] E. W. Leaver, Proc. R. Soc. A **402**, 285 (1985).
[77] R. A. Konoplya and A. Zhidenko, Rev. Mod. Phys. **83**, 793 (2011).
[78] Y. Hatsuda and M. Kimura, Phys. Rev. D **109**, 044026 (2024).
[79] https://github.com/JialeZHANG-Phys/pqnm_overtone
[80] M. Kimura, Phys. Rev. D **101**, 064031 (2020).
[81] B. F. Schutz and C. M. Will, Astrophys. J. Lett. **291**, L33 (1985).
[82] S. Endlich, V. Gorbenko, J. Huang, and L. Senatore, J. High Energy Phys. 09 (2017) 122.
[83] V. Cardoso, M. Kimura, A. Maselli, and L. Senatore, Phys. Rev. Lett. **121**, 251105 (2018); **131**, 109903(E) (2023).
[84] P. A. Cano and A. Ruipérez, J. High Energy Phys. 05 (2019) 189; 03 (2020) 187.
[85] K. Nomura and D. Yoshida, Phys. Rev. D **105**, 044006 (2022).
[86] P. A. Cano, B. Ganchev, D. R. Mayerson, and A. Ruipérez, J. High Energy Phys. 12 (2022) 120.
[87] H. O. Silva, A. Ghosh, and A. Buonanno, Phys. Rev. D **107**, 044030 (2023).

[88] P. A. Cano, K. Fransen, T. Hertog, and S. Maenaut, Phys. Rev. D **108**, 124032 (2023).
[89] R. Cayuso, P. Figueras, T. França, and L. Lehner, Phys. Rev. Lett. **131**, 111403 (2023).
[90] P. A. Cano, K. Fransen, T. Hertog, and S. Maenaut, Phys. Rev. D **108**, 024040 (2023).
[91] S. Melville, arXiv:2401.05524.
[92] N. Sennett, R. Brito, A. Buonanno, V. Gorbenko, and L. Senatore, Phys. Rev. D **102**, 044056 (2020).
[93] C. Y. R. Chen, C. de Rham, A. Margalit, and A. J. Tolley, J. High Energy Phys. 03 (2022) 025.
[94] C. de Rham, A. J. Tolley, and J. Zhang, Phys. Rev. Lett. **128**, 131102 (2022).
[95] F. Serra, J. Serra, E. Trincherini, and L. G. Trombetta, J. High Energy Phys. 08 (2022) 157.
[96] M. Carrillo González, C. de Rham, S. Jaitly, V. Pozsgay, and A. Tokareva, arXiv:2307.04784.
[97] M. B. Green and J. H. Schwarz, Phys. Lett. **149B**, 117 (1984).
[98] R. R. Metsaev and A. A. Tseytlin, Nucl. Phys. **B293**, 385 (1987).
[99] I. Antoniadis, E. Gava, and K. S. Narain, Phys. Lett. B **283**, 209 (1992).
[100] S. Mignemi and N. R. Stewart, Phys. Rev. D **47**, 5259 (1993).
[101] S. Mignemi, Phys. Rev. D **51**, 934 (1995).
[102] I. Antoniadis, J. Rizos, and K. Tamvakis, Nucl. Phys. **B415**, 497 (1994).
[103] P. Kanti, N. E. Mavromatos, J. Rizos, K. Tamvakis, and E. Winstanley, Phys. Rev. D **54**, 5049 (1996).
[104] J. L. Blázquez-Salcedo, C. F. B. Macedo, V. Cardoso, V. Ferrari, L. Gualtieri, F. S. Khoo, J. Kunz, and P. Pani, Phys. Rev. D **94**, 104024 (2016).
[105] S. Hirano, M. Kimura, and M. Yamaguchi, Phys. Rev. D **109**, 124022 (2024).
[106] N. Yunes and L. C. Stein, Phys. Rev. D **83**, 104002 (2011).
[107] G. B. Cook and M. Zalutskiy, Phys. Rev. D **90**, 124021 (2014).
[108] G. B. Cook, https://zenodo.org/records/10093311.
[109] S. Chandrasekhar and S. L. Detweiler, Proc. R. Soc. A **350**, 165 (1976).
[110] S. L. Detweiler, Proc. R. Soc. A **352**, 381 (1977).
[111] V. Cardoso, S. Kastha, and R. Panosso Macedo, arXiv: 2404.01374.
[112] R. J. Gleiser, C. O. Nicasio, R. H. Price, and J. Pullin, Classical Quantum Gravity **13**, L117 (1996).
[113] M. Campanelli and C. O. Lousto, Phys. Rev. D **59**, 124022 (1999).
[114] Y. Zlochower, R. Gomez, S. Husa, L. Lehner, and J. Winicour, Phys. Rev. D **68**, 084014 (2003).
[115] K. Ioka and H. Nakano, Phys. Rev. D **76**, 061503 (2007).
[116] H. Nakano and K. Ioka, Phys. Rev. D **76**, 084007 (2007).
[117] D. Brizuela, J. M. Martin-Garcia, and M. Tiglio, Phys. Rev. D **80**, 024021 (2009).
[118] E. Pazos, D. Brizuela, J. M. Martin-Garcia, and M. Tiglio, Phys. Rev. D **82**, 104028 (2010).
[119] N. Loutrel, J. L. Ripley, E. Giorgi, and F. Pretorius, Phys. Rev. D **103**, 104017 (2021).
[120] J. L. Ripley, N. Loutrel, E. Giorgi, and F. Pretorius, Phys. Rev. D **103**, 104018 (2021).
[121] L. Sberna, P. Bosch, W. E. East, S. R. Green, and L. Lehner, Phys. Rev. D **105**, 064046 (2022).
[122] S. Ma, K. Mitman, L. Sun, N. Deppe, F. Hébert, L. E. Kidder, J. Moxon, W. Throwe, N. L. Vu, and Y. Chen, Phys. Rev. D **106**, 084036 (2022).
[123] N. Khera, A. Ribes Metidieri, B. Bonga, X. Jiménez Forteza, B. Krishnan, E. Poisson, D. Pook-Kolb, E. Schnetter, and H. Yang, Phys. Rev. Lett. **131**, 231401 (2023).
[124] M. Lagos and L. Hui, Phys. Rev. D **107**, 044040 (2023).
[125] T. Guerreiro, arXiv:2306.09974.
[126] A. Kehagias, D. Perrone, A. Riotto, and F. Riva, Phys. Rev. D **108**, L021501 (2023).
[127] A. Kehagias and A. Riotto, arXiv:2302.01240.
[128] J. Redondo-Yuste, G. Carullo, J. L. Ripley, E. Berti, and V. Cardoso, Phys. Rev. D **109**, L101503 (2024).
[129] D. Perrone, T. Barreira, A. Kehagias, and A. Riotto, Nucl. Phys. **B999**, 116432 (2024).
[130] B. Bucciotti, A. Kuntz, F. Serra, and E. Trincherini, J. High Energy Phys. 12 (2023) 048.
[131] S. Ma and H. Yang, Phys. Rev. D **109**, 104070 (2024).
[132] S. Yi, A. Kuntz, E. Barausse, E. Berti, M. H. Y. Cheung, K. Kritos, and A. Maselli, arXiv:2403.09767.
[133] M. Okounkova, arXiv:2004.00671.
[134] Y. Hatsuda, Gen. Relativ. Gravit. **53**, 93 (2021).
[135] A. Maassen van den Brink, Phys. Rev. D **62**, 064009 (2000).
[136] E. Berti, V. Cardoso, and A. O. Starinets, Classical Quantum Gravity **26**, 163001 (2009).
[137] E. Berti, V. Cardoso, K. D. Kokkotas, and H. Onozawa, Phys. Rev. D **68**, 124018 (2003).
[138] G. B. Cook and M. Zalutskiy, Classical Quantum Gravity **33**, 245008 (2016).
[139] G. B. Cook and M. Zalutskiy, Phys. Rev. D **94**, 104074 (2016).